

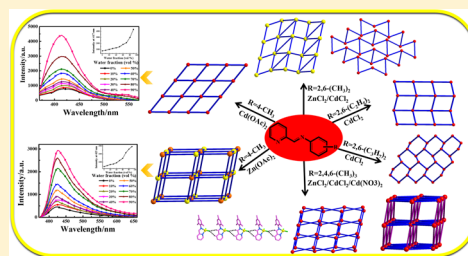
(*E*)-*N*-(Pyridine-2-ylmethylene)arylamine as an Assembling Ligand for Zn(II)/Cd(II) Complexes: Aryl Substitution and Anion Effects on the Dimensionality and Luminescence Properties of the Supramolecular Metal–Organic Frameworks

Yu-Wei Dong,[†] Rui-Qing Fan,^{*,†} Xin-Ming Wang,[†] Ping Wang,[†] Hui-Jie Zhang,[†] Li-Guo Wei,[†] Wei Chen,[†] and Yu-Lin Yang^{*,†}

[†]MITT Key Laboratory of Critical Materials Technology for New Energy Conversion and Storage, School of Chemistry and Chemical Engineering, Harbin Institute of Technology, Harbin 150001, P. R. of China

S Supporting Information

ABSTRACT: Using five Schiff base ligands (*E*)-*N*-(pyridine-2-yl) (CH=NPhR) (where R = 4-CH₃, L¹; 2,6-(CH₃)₂, L²; 2,4,6-(CH₃)₃, L³; 2,6-(C₂H₅)₂, L⁴; 2,6-(*i*-C₃H₇)₂, L⁵), nine Zn(II)/Cd(II) complexes, namely, Zn1–Zn3, Cd1, Cd2, Cd3a, Cd3b, Cd4, and Cd5, have been successfully synthesized. The structures of the Zn(II)/Cd(II) complexes have been established by single crystal X-ray diffraction and further physically characterized by ¹H NMR, FT-IR, and elemental analysis. The crystal structures of these complexes indicate that the structures of ligand and anions can directly influence the formation of 1D → 3D supramolecular metal–organic frameworks (SMOFs) via C–H⋯O/C–H⋯Cl hydrogen bonds and π⋯π interactions. Upon irradiation with UV light, the nine Zn(II)/Cd(II) complexes display deep blue emissions of 401–436 nm in acetonitrile solution and light blue or bluish green emissions of 485–575 nm in the solid state, respectively. The photoluminescence properties of nine Zn(II)/Cd(II) complexes can be finely and predictably tuned over a wide range of wavelengths by small and easily implemented changes to ligand structure. It is worth noting that Zn1 and Cd1 exhibit obvious aggregation-induced emission enhancement (AIEE) properties in the CH₃CN–H₂O mixture solutions.



■ INTRODUCTION

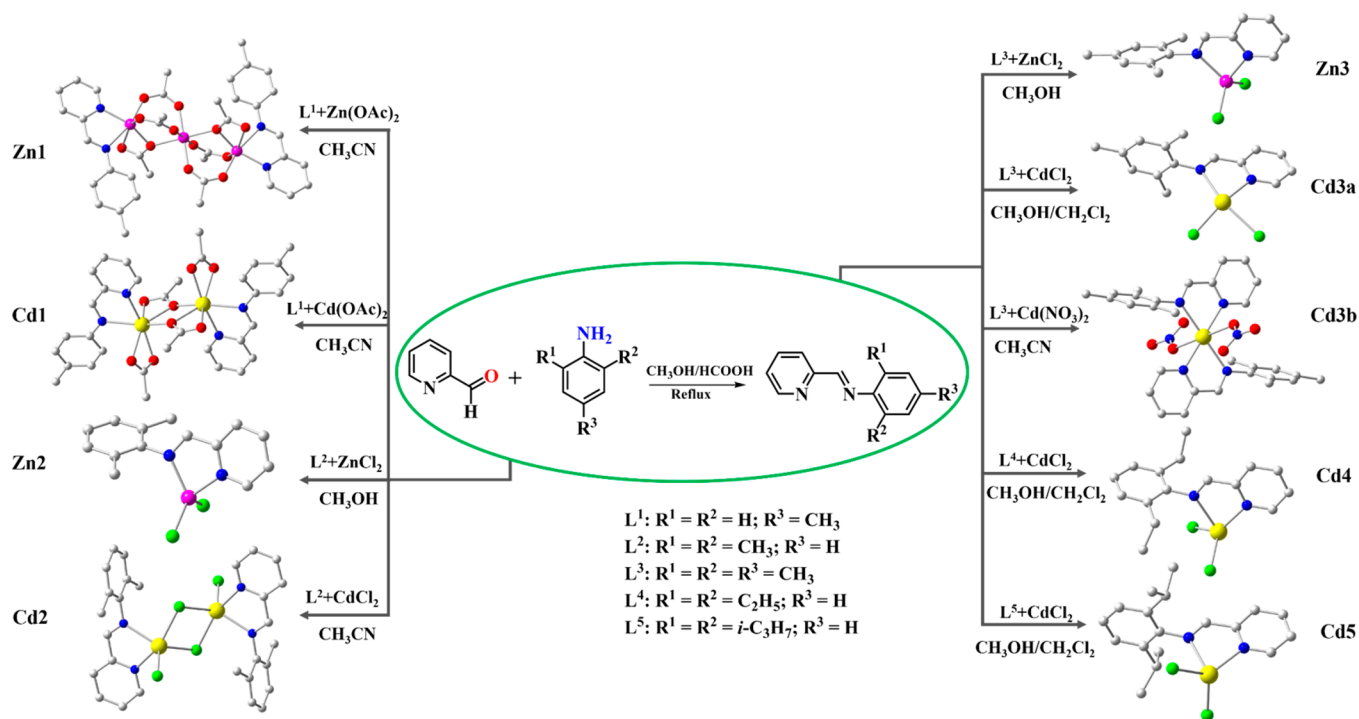
Over the past decade, supramolecular chemistry of coordination compounds has attracted great interest due to their intriguing structures and wide potential applications in different areas, such as nonlinear optics, magnetism, photoluminescence, and electrochemistry.^{1–8} These functional materials are generally constructed by covalent and noncovalent interactions.^{9,10} The type of noncovalent supramolecular interaction, such as hydrogen bonding,^{11–14} and π⋯π stacking,^{15–19} depends on the shape and functional groups of the components that form supramolecular metal–organic frameworks (SMOFs). It is noteworthy that the appropriate hydrogen bonding and π⋯π stacking interactions could produce the aggregation-induced emission phenomenon, which was first reported by Tang et al. in 2001.²⁰ Therefore, this superiority in the solid state materials significantly expands the real-world applications if they possess aggregation-induced emission in the solid or aggregated state. These functional materials are generally constructed by metal ions and bridging organic ligands.²¹ The ligand not only provides capability for selective metal ion coordination but also generates desired noncovalent intermolecular interactions to direct crystal packing.^{22–24} Hence, the major challenge of supramolecular chemistry lies in the rewarding endeavors to design and synthesize organic ligands. Schiff base ligands play an important role in metal

coordination chemistry, even after almost a century since their discovery, this is attributed to their facile synthesis, remarkable versatility, and good solubility in common solvents.^{25–27} In general, compared with rigid ligands, a metal-coordinated Schiff base ligand can readily form intermolecular π⋯π or C–H⋯π interactions in the aggregated or crystal state because of the high flexibility of the imine unit.

The assembly process of the complex can be affected by many factors; among them, the metal ions, anions, and ligands are base-control factors.^{28,29} It is well-known that different metal ions possess different properties and coordination modes, which play key roles in the formation of both molecular structures and packing structures of complexes. For example, Zn(II) and Cd(II) ions often adopt different coordination modes, such as four-, five-, six-, or seven-coordination modes when they react with organic ligands.^{30–33} The introducing of different small anions can also have a significant effect on the structural construction of complexes and their properties. In coordination chemistry, halogen, acetate, and nitrate ions have been widely used as anions for the construction of the metal coordination complexes because they can adjust the topologies

Received: March 3, 2016

Revised: May 3, 2016

Scheme 1. Syntheses Routes of Five Ligands L¹–L⁵ and Nine Corresponding Zn(II)/Cd(II) Complexes

of complexes through different covalent bonds or noncovalent interactions.^{34,35}

Inspired by the above discussion, herein, five Schiff base ligands (*E*)-*N*-(pyridine-2-yl)(CH=NPhR), L¹–L⁵, Scheme 1, carrying different alkyl substitutions in the phenyl ring have been employed for the synthesis of Zn(II)/Cd(II) complexes. Nine Zn(II)/Cd(II) complexes, namely Zn1–Zn3, Cd1, Cd2, Cd3a, Cd3b, Cd4, and Cd5, were prepared by the reaction of corresponding ligand and M(II) salts. Subsequently, the structures of ligands and Zn(II)/Cd(II) complexes have been characterized by means of ¹H NMR, IR, and EA spectroscopic studies, and for complexes Zn1–Zn3, Cd1, Cd2, Cd3a, Cd3b, Cd4, and Cd5 additionally by single-crystal X-ray crystallography. The structure of complex Zn2 has been reported by Zhao et al.,³⁶ and there existed similar complexes in the literature,^{37,38} but they simply show the structure of the unit cell rather than intermolecular interactions. Herein, we systematically investigated the effect of related alkyl substitution Schiff base ligands and intermolecular interactions (C–H⋯O/C–H⋯Cl hydrogen bonds and π⋯π interactions) in the organization and stabilization of supramolecular metal–organic frameworks (SMOFs). Moreover, the influence of the substituent effect on the photoluminescence in CH₃CN solution and the solid state was discussed. Complexes Zn1 and Cd1 exhibit aggregation-induced emission enhancement (AIEE) behavior in CH₃CN/H₂O solutions.

RESULTS AND DISCUSSION

Synthesis and spectral characterization. The five imine ligands (*E*)-*N*-(pyridine-2-yl)(CH=NPhR) (where R = 4-CH₃, L¹; 2,6-(CH₃)₂, L²; 2,4,6-(CH₃)₃, L³; 2,6-(C₂H₅)₂, L⁴; 2,6-(*i*-C₃H₇)₂, L⁵) were readily prepared in a one-step procedure by condensation of 2-pyridinecarboxaldehyde with the corresponding monamine in a 1:1 molar ratio in anhydrous methanol/formic acid solution (see Scheme 1). Moreover, the yellow bulk crystals of L¹ were obtained by recrystallization

from the mixed solvent of *n*-hexane and dichloromethane. L³ and L⁵ were recrystallized from *n*-hexane to give yellow crystals. Yields for the five imine ligands varied from 70 to 91%. Using a self-assembled method, these ligands were reacted with Zn(II)/Cd(II) salts to obtain a series of complexes, namely, Zn1–Zn3, Cd1, Cd2, Cd3a, Cd3b, Cd4, and Cd5. X-ray quality single crystals of nine Zn(II)/Cd(II) complexes were grown from slow evaporation of their solutions and were readily obtained in good yields within the range 56–72%. The details of the synthesis are given in the Experimental Section. We confirm that all the complexes are stable in the solid state under exposure to air. The complexes are soluble in common organic solvents, such as chloroform, dimethyl sulfoxide, and acetonitrile.

The infrared spectra of these nine Zn(II)/Cd(II) complexes (see Figures S1–S5 in the Supporting Information) are similar to that of the corresponding ligand, and the IR assignments of selected diagnostic bands are given in the Experimental Section. In the IR spectra of ligands L¹–L⁵, the existence of C=N bonds is clearly demonstrated by the presence of strong characteristic C=N peaks in the range 1628–1668 cm⁻¹. These bands undergo negative shifts of 2–39 cm⁻¹ in the complexes, which may be attributed to the coordination of the nitrogen atom of the imine to the metal ion.^{39,40} This is further confirmed by the presence of a ν(M–N) vibration in the region 422–454 cm⁻¹ in all the complexes.⁴¹ The ¹H NMR spectra of the imine ligands L¹–L⁵ and its Zn(II)/Cd(II) complexes were recorded in CDCl₃ at room temperature (see Figures S6–S10 in the Supporting Information). In the ¹H NMR spectra, the chemical shift values of the protons in the complexes are slightly different from those observed for the noncoordinated ligand. Of particular note is the HC=N resonances of the nine Zn(II)/Cd(II) complexes, which are moved downfield due to coordination between the imine nitrogen and the M(II) center.⁴² For the complexes, the imine proton is moved downfield at most 0.10 ppm. Meanwhile, the resonance peaks

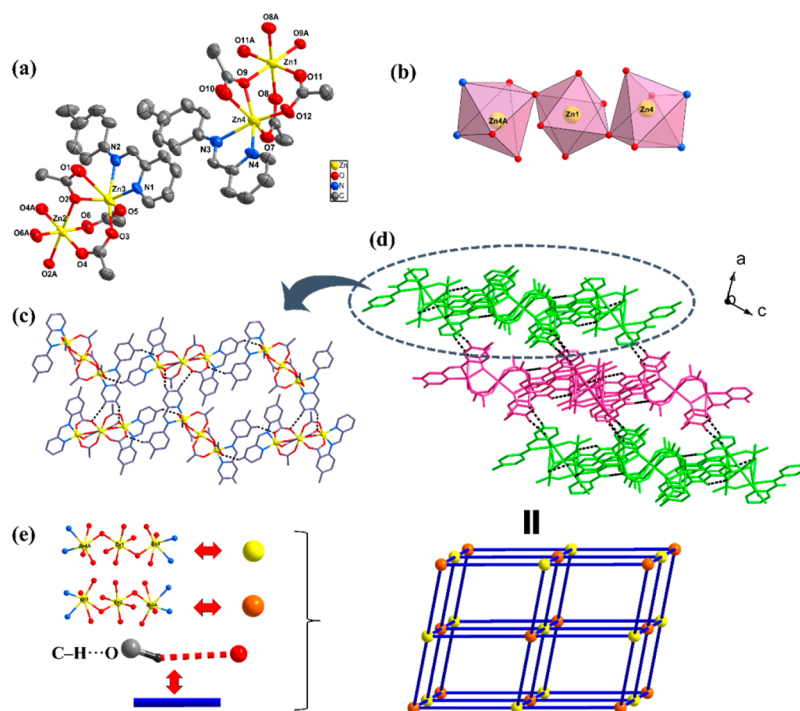


Figure 1. (a) Asymmetric unit cell of **Zn1**. The thermal ellipsoid is drawn at 50% probability. H atoms have been omitted for clarity. (b) Polyhedral representation of the coordination sphere of the Zn(II) center in **Zn1**. (c) The 2D layer and (d) 3D network structure in **Zn1**. Dotted lines represent the C–H \cdots O interactions. (e) Topological view of the 3D network structure of **Zn1**.

at 1.82 (**Zn1**) and 2.04 (**Cd1**) ppm are assigned to $-\text{CH}_3\text{COO}$ protons. To further understand the structures of these complexes, single crystals were obtained and analyzed by single crystal X-ray diffraction. The crystallographic data for these nine Zn(II)/Cd(II) complexes are listed in Table S1, [Supporting Information](#).

Description of the structures. Structural analysis of Zn1 and Cd1. Complex $[\text{Zn}_3(\text{L}^1)_2(\text{OAc})_6]$ (**Zn1**) crystallized in the triclinic space group $P\bar{1}$. There exist two identical half molecules. As shown in [Figure 1a](#), for a complete molecule, two equivalent $[\text{Zn}(\text{L}^1)]$ moieties are bridged to the central Zn^{2+} ion (Zn1) by two $\mu_2\text{-}\eta_0^1\text{-}\eta_0^2$ OAc^- anions and four $\mu_2\text{-}\eta_0^1\text{-}\eta_0^1$ OAc^- anions, resulting in the formation of a trinuclear structure. The two terminal Zn^{2+} ions, Zn4 and Zn4A, are six-coordinated with one N atom (N4) from one chelating ligand L^1 and three O atoms (O7, O9, and O10) from the coordinated OAc^- anion to constitute the equatorial plane, and one N atom (N3) and one O atom (O4) at the axial position, resulting in a distorted octahedral geometry ([Figure 1b](#)). The central Zn^{2+} ion (Zn1) is six-coordinated with six O atoms (O8, O8A, O9, O9A, O11, and O11A) from four OAc^- anions. The intermetallic Zn(1) \cdots Zn(4) and Zn(2) \cdots Zn(3) distances are 3.397(12) and 3.382(14) Å, respectively. The ligand (L^1) is approximately planar (the dihedral angles between the pyridyl and phenyl rings: $6.053^\circ/10.027^\circ$, [Table 1](#)) and coordinates to the Zn via a bidentate N,N interaction. In complex **Zn1**, the independent units are linked through C3–H3A \cdots O10, C22–H22A \cdots O1, C23–H23A \cdots O6, and C30–H30A \cdots O5 hydrogen bond interactions to generate a two-dimensional layer ([Figure 1c](#)). The H3A \cdots O10, H22A \cdots O1, H23A \cdots O6, and H30A \cdots O5 distances are 2.444, 2.478, 2.575, and 2.485 Å, respectively. The two-dimensional layer further extends into the three-dimensional supramolecular network through C6–H6A \cdots O7, C21–H21A \cdots O1, and C25–H25A \cdots O1 hydrogen bond interactions,

as shown in [Figure 1d](#). If the two separated trinuclear units are viewed as two different nodes and the hydrogen bonds C–H \cdots O as the linkers, the resulting (6,6)-connected three-dimensional supramolecular structure may be simplified by the Schläfli symbol $\{4^{12}\cdot 6^3\}$, as depicted in [Figure 1e](#).

The asymmetric unit of complex $[\text{CdL}^1(\text{OAc})_2]$ (**Cd1**) consists of one crystallographically independent Cd^{2+} cation, one ligand L^1 , and two OAc^- anions ([Figure 2a](#)). Every Cd^{2+} cation is seven-coordinated with slightly distorted pentagonal bipyramid coordination geometry $[\text{CdN}_2\text{O}_5]$, containing two N atoms (N1 and N2) from L^1 , and five O atoms (O1, O2, O3, O3A, and O4) from OAc^- anions. Two equivalent $[\text{Cd}(\text{L}^1)]$ moieties are linked via O3 and O3A atoms to form a binuclear structure. The intermetallic Cd(1) \cdots Cd(1A) distance is 3.821(6) Å. The distances of Cd1–N1 and Cd1–N2 are 2.327(2) and 2.416(2) Å, which are in agreement with the values of a similar cadmium complex.⁴³ The detailed bond distances and angles for **Cd1** are listed in Table S2, [Supporting Information](#). The adjacent binuclear molecules are interconnected through C6–H6A \cdots O4 and C8–H8A \cdots O4 hydrogen bond interactions to form a 1D chain ([Figure 2b](#)). The H6A \cdots O4 and H8A \cdots O4 distances are 2.452 and 2.695 Å, respectively. Two adjacent chains are interconnected via C3–H3A \cdots O2 hydrogen bond interactions ($d_{\text{H3A}\cdots\text{O2}} = 2.533$ Å) to construct a 2D layer. From the topological point of view, the binuclear unit could be considered as the node, and hydrogen bonds C–H \cdots O could be considered as the linkers. Thus, the two-dimensional net of **Cd1** can be described as a 4-connected *sql* net with the Schläfli symbol $\{4^4\cdot 6^2\}$ ([Figure 2c](#)).

Structural analysis of Zn2 and Cd2. The N atoms of ligand L^2 are coordinated with $\text{ZnCl}_2/\text{CdCl}_2$ to form mononuclear $[\text{ZnL}^2\text{Cl}_2]$ (**Zn2**) and binuclear $[\text{CdL}^2\text{Cl}_2]_2$ (**Cd2**), respectively, as shown in [Figure 3a](#) and [3b](#). Using Addison's model,^{44,45} the coordination geometry around the zinc atom

Table 1. Structural and Geometrical Parameters for Complexes Zn1–Zn3, Cd1, Cd2, Cd3a, Cd3b, Cd4, and Cd5

Complex	coordination number	coordination geometry	Addison parameter (τ)	dihedral angle (deg) ^a	D–H \cdots A	D–H (Å)	H \cdots A (Å)	D \cdots A (Å)	D–H \cdots A (deg)	dimension
Zn1	6	octahedral		6.053, 10.027	C3–H3A \cdots O10	0.930	2.444	3.176	135.585(2)	3D
					C6–H6A \cdots O7	0.930	2.630	3.447	146.937(2)	
					C21–H21A \cdots O1	0.930	2.550	3.326	141.171(4)	
					C22–H22A \cdots O7	0.930	2.478	3.314	149.663(2)	
					C23–H23A \cdots O6	0.930	2.575	3.432	153.259(4)	
					C25–H25A \cdots O1	0.930	2.494	3.277	141.982(2)	
					C30–H30A \cdots O5	0.930	2.485	3.343	153.536(2)	
Cd1	7	pentagonal bipyramid		14.226	$\pi_{C_{g1}^b} \cdots \pi_{C_{g2}^c}$			3.952		2D
					C3–H3A \cdots O1	0.930	2.533	3.330	143.966(1)	
					C6–H6A \cdots O4	0.930	2.452	3.365	167.071(1)	
					C8–H8A \cdots O4	0.930	2.695	3.440	137.694(1)	
Zn2	4	tetrahedral	0.831	64.315	$\pi_{C_{g1}^b} \cdots \pi_{C_{g2}^c}$			3.633		2D
					C2–H2A \cdots Cl1	0.930	2.888	3.703	147.170(1)	
					C5–H5A \cdots Cl2	0.930	2.898	3.642	137.859(1)	
					C6–H6A \cdots Cl1	0.930	2.781	3.610	149.051(1)	
Cd2	5	trigonal bipyramidal	0.543	85.649	C10–H10A \cdots Cl2	0.930	2.946	3.839	161.617(1)	2D
					$\pi_{C_{g1}^b} \cdots \pi_{C_{g1}^c}$			3.889		
					C2–H2A \cdots Cl1	0.930	2.919	3.650	136.452(5)	
					C4–H4A \cdots Cl2	0.930	2.927	3.572	127.595(4)	
Zn3	4	tetrahedral	0.848	73.266	C2–H2A \cdots Cl1	0.930	2.860	3.684	148.410(3)	1D
					C6–H6A \cdots Cl1	0.930	2.889	3.701	146.586(2)	
Cd3a	4	tetrahedral	0.494	82.952	$\pi_{C_{g1}^b} \cdots \pi_{C_{g1}^c}$			3.715		2D
					C4–H4A \cdots Cl2	0.929	2.903	3.820	169.481(2)	
					C5–H5A \cdots Cl2	0.929	2.896	3.558	129.263(1)	
					C6–H6A \cdots Cl1	0.930	2.822	3.420	123.089(1)	
Cd3b	6	octahedral		72.072	C15–H15B \cdots Cl1	0.960	2.746	3.636	154.669(1)	3D
					$\pi_{C_{g1}^b} \cdots \pi_{C_{g2}^c}$			3.518		
					C2–H2A \cdots O3	0.930	2.642	3.397	138.722(2)	
					C6–H6A \cdots O3	0.930	2.454	3.276	147.361(1)	
Cd4	4	tetrahedral	0.760	82.240	C11–H11A \cdots O2	0.930	2.518	3.348	148.853(2)	2D
					C13–H13C \cdots O2	0.961	2.593	3.395	141.156(2)	
					C2–H2A \cdots Cl1	0.930	2.891	3.735	151.395(1)	
Cd5	4	tetrahedral	0.737	85.110	C4–H4A \cdots Cl2	0.930	2.927	3.593	129.647(1)	2D
					C6–H6A \cdots Cl1	0.930	2.794	3.657	154.699(1)	
					C5–H5A \cdots Cl2	0.930	2.890	3.474	121.964(1)	
					C6–H6A \cdots Cl1	0.930	2.711	3.593	158.565(1)	

^aBetween the pyridyl ring and phenyl ring. ^b C_{g1} = pyridyl ring. ^c C_{g2} = phenyl ring.

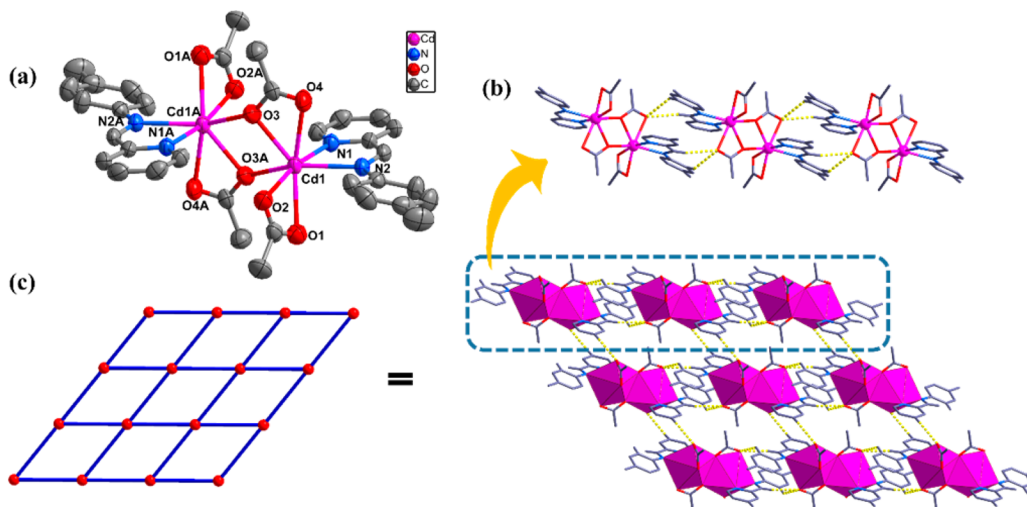


Figure 2. (a) Crystal structure of Cd1. The thermal ellipsoid is drawn at 50% probability. H atoms have been omitted for clarity. (b) The 1D chain structure in Cd1. (c) The 2D layer structure and topological view in Cd1. Dotted lines represent the C–H \cdots O interactions.

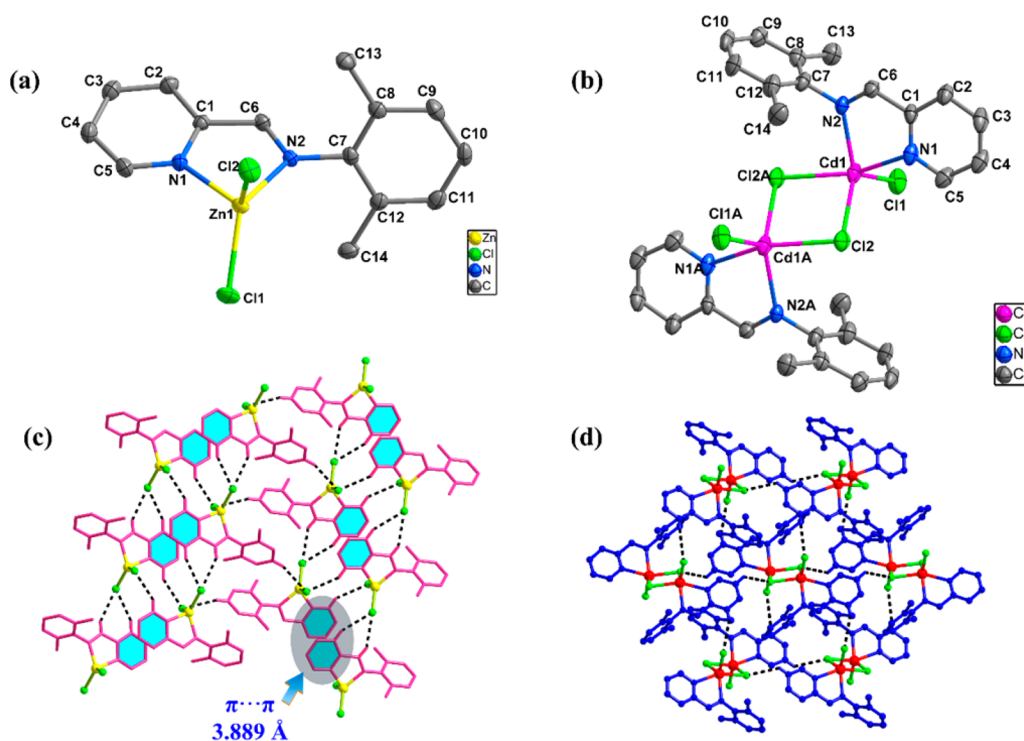


Figure 3. Crystal structures of (a) **Zn2** and (b) **Cd2**. The thermal ellipsoid is drawn at 50% probability. H atoms have been omitted for clarity. The 2D layer structures of (c) **Zn2** and (d) **Cd2**. Dotted lines represent the C–H \cdots Cl interactions.

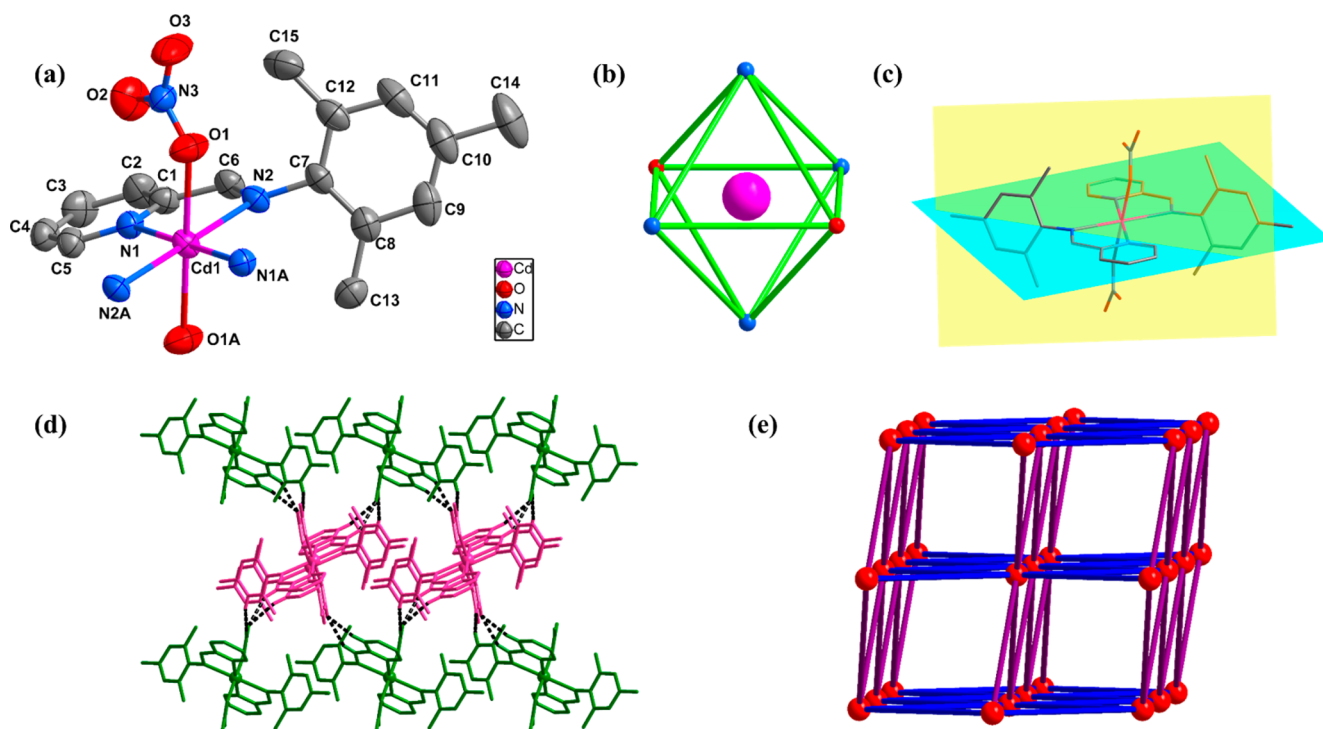


Figure 4. (a) Asymmetric unit cell of **Cd3b**. The thermal ellipsoid is drawn at 50% probability. H atoms have been omitted for clarity. (b) Coordination geometry of cadmium(II) ions. (c) Depiction of the dihedral angle between the pyridine ring and the phenyl ring in **Cd3b**. (d) The 3D network structure of and (e) topological view in **Cd3b**. Dotted lines represent the C–H \cdots O interactions.

in **Zn2** ($\tau_4 = 0.831$) and the cadmium atom in **Cd2** ($\tau_5 = 0.543$) can be better described as a tetrahedral and trigonal bipyramidal, respectively. The X-ray single crystal structure of **Cd2** consists of half of the neutral binuclear molecule, with the other half obtained by a center of inversion. The binuclear

moiety contains two Cd(II) atoms (Cd1 and Cd1A), which are asymmetrically bridged by two chloride anions (Cl1 and Cl1A), while the molecule of the bidentate L^2 ligand is N-coordinated to each cadmium atom. The separation of intramolecular Cd1 \cdots Cd1A is 3.695(14) Å. The dihedral angles between the pyridine

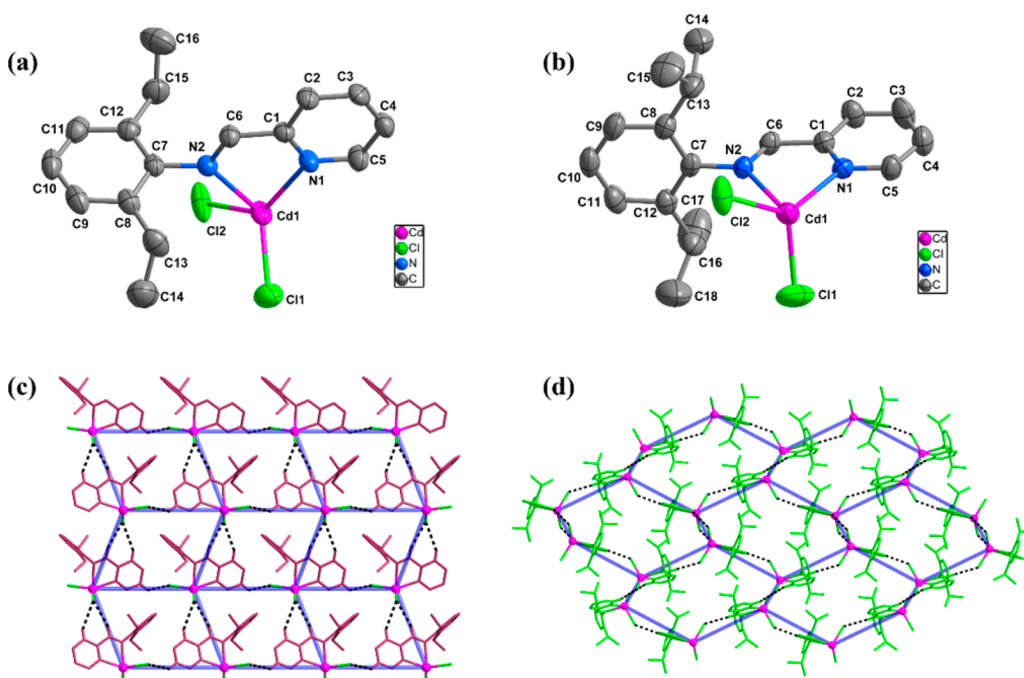


Figure 5. Crystal structures of (a) Cd4 and (b) Cd5. The thermal ellipsoid is drawn at 50% probability. H atoms have been omitted for clarity. The 2D layer structures of (c) Cd4 and (d) Cd5. Dotted lines represent the C–H \cdots Cl interactions.

ring and the phenyl ring are 64.315° (Zn2) and 85.649° (Cd2), which is very twisted compared with the complexes of the ligand L^1 . Likewise, the distances of M–N (imino) are relatively shorter than M–N (pyridine). The average distances of the M–N bonds are 2.068 \AA (Zn2) and 2.354 \AA (Cd2), which is consistent with ionic radii. The selected bond lengths and bond angles of complexes Zn2 and Cd2 are given in Table S3, Supporting Information, respectively. Single crystal analysis shows that complexes Zn2 and Cd2 are both two-dimensional layer structures (Figures 3c and 3d, respectively) constructed by the C–H \cdots Cl (Table 1) hydrogen bond interactions.⁴⁶ Significantly, additional intermolecular $\pi\cdots\pi$ interactions with separations of about 3.889 \AA (Figure 3c) also provide further stabilization in complex Zn2. The resulting two-dimensional nets may be simplified into a 2D 5-connected *cem* topology with the Schläfli symbol $\{3^3\cdot 4^4\cdot 5^3\}$ for Zn2, and a 2D 3-connected *hcb* topology with the Schläfli symbol $\{6^3\}$ for Cd2, as shown in Figures S11a and S11b, respectively.

Structural analysis of Zn3, Cd3a, and Cd3b. As shown in Figures S12a and S12b, the complexes $[\text{ZnL}^3\text{Cl}_2]$ (Zn3) and $[\text{CdL}^3\text{Cl}_2]$ (Cd3a) are isostructural, so we choose Cd3a to represent the detailed structure. They all belong to the monoclinic $P2_1/c$ space group. In complex Cd3a, the Cd(II) center adopts a distorted tetrahedral geometry ($\tau_4 = 0.494$, Cd3a; 0.848 , Zn3) coordinated by two nitrogen atoms of (*E*)-2,4,6-trimethyl-*N*-((pyridin-2-yl)methylene)aniline (L^3) and two terminal chlorine ions. In particular, the Cd(II) cation coordinates with nitrogen atoms from ligand L^3 to form a five-membered ring, which further extends system conjugation. Complexes Zn3 and Cd3a have dihedral angles of 73.266° and 82.952° , respectively, between the pyridyl ring and the phenyl ring (Table 1), which indicates that the ligand L^3 is very twisted in Zn3 and Cd3a. In addition, the mononuclear units of Zn3 and Cd3a are further assembled into a 1D chain and 2D net by C–H \cdots Cl hydrogen bond interactions (the detailed data of C–H \cdots Cl hydrogen bonds for Zn3 and Cd3a are listed in Table

1), and the resulting Cd3a two-dimensional nets may be simplified into a 2D 5-connected $\{4^6\cdot 5^2\cdot 6^2\}$ topology, as shown in Figures S13a and S13b, respectively.

Single crystal analysis reveals that complex $[\text{Cd}(\text{L}^3)_2(\text{NO}_3)_2]$ (Cd3b) crystallizes in a monoclinic system, space group $P2_1/n$. As shown in Figure 4a, the central metal Cd(II) ion is six coordinated by two O atoms from two nitrate anions and by four N atoms from two ligands, to form a distorted octahedral geometry (Figure 4b). The bond angles around the Cd(II) ion are in the range $72.84(7)$ – $180.00(14)^\circ$. The selected bond distances and angles are shown in Table S4, Supporting Information. The dihedral angles between the pyridine ring and the phenyl ring in the Cd3b (72.072°) are approximately perpendicular (Figure 4c). Similar to Zn1 and Cd1, C–H \cdots O hydrogen bond interactions based on the O atom of the coordination anions are formed. As shown in Figure 4d, two adjacent molecules are linked by the C2–H2A \cdots O3, C6–H6A \cdots O3, and C11–H11A \cdots O2 hydrogen bond interactions to form a 3D SMOF. The H2A \cdots O3, H6A \cdots O3, and H11A \cdots O2 distances are 2.642 , 2.454 , and 2.518 \AA , respectively. In addition, the hydrogen bonding interactions (C13–H13C \cdots O2) based on intramolecules provide further stability to the 3D structure. The resulting three-dimensional supramolecular structure may be simplified into a 3D 8-connected *bcu* topology with the Schläfli symbol $\{4^{24}\cdot 6^4\}$ (Figure 4e).

Structural analysis of Cd4 and Cd5. Both complexes Cd4 and Cd5 crystallize in the monoclinic $P2_1/n$ space group. The asymmetric unit of Cd4 consists of one independent Cd(II) ion, one whole ligand L^4 , and two chlorine anions. The coordination pattern of Cd5 is similar to that of Cd4, except for L^5 being used instead of L^4 . As shown in Figures 5a and 5b, the Cd(II) ions in Cd4 and Cd5 are located in a distorted tetrahedral coordination geometry with τ_4 parameters 0.760 and 0.737 , respectively. The Cd–N bond lengths in Cd4 vary from $2.316(19)$ to $2.396(2) \text{ \AA}$, and Cd–Cl bond lengths vary from $2.423(10)$ to $2.524(12) \text{ \AA}$, whereas these geometric

parameters vary from 2.316(2) to 2.402(2) Å and from 2.416(11) to 2.516(9) Å in Cd5, respectively (Table S5, Supporting Information). The pyridyl and phenyl rings of dihedral angles are 82.240° in Cd4 and 85.110° in Cd5, respectively. Regarding the C–H⋯Cl hydrogen bond interactions as linkers, and the mononuclear unit in Cd4 and Cd5 as a 4-connected and a 3-connected node, respectively, Cd4 exhibits 2D *sql* topology with the Schläfli symbol {4⁴.6²}, and a 2D *hcb* topology with the Schläfli symbol {6³} for Cd5. The detailed data of C–H⋯Cl hydrogen bonds for Cd4 and Cd5 are listed in Table 1.

Effect of aryl substitution and anion on supramolecular architecture. In this article, we have successfully synthesized a series of Zn/Cd(II) SMOFs via the hydrogen bonding interaction by the method of changing the aryl substitution and anion.

Taking the structures into account, there exists a dramatic influence of the aryl substitutions on the steric hindrance of the complexes. With increased numbers of methyl substituents on the ligands, the steric hindrance of the complexes gradually increases [dihedral angles: 6.053° and 10.027°, Zn1 (2-CH₃); 64.315°, Zn2 (2,6-(CH₃)₂); 73.266°, Zn3 (2,4,6-(CH₃)₃)], which results in 3D → 1D supramolecular architectures. That is to say, the complexes display better coplanarity with decreasing numbers of methyl substituents. The larger steric hindrance of ligands could hinder molecular assemblies and influence the form of supramolecular architectures. In addition, the ligands with 2,6-(CH₃)₂, 2,6-(C₂H₅)₂, and 2,6-(*i*-C₃H₇)₂ substituents in the same position also augment the steric hindrance; however, there seems to be little influence on constructing the supramolecular architectures. With careful observation, we find that most hydrogen bonding interactions concentrate on the pyridine ring. Thus, the influence of different substituents in the same position of the ligands is smaller than that of the numbers of methyl substituents on the ligand.

On the other hand, although most of the complexes are made by chloride as metal source, but through the hydrogen bonding interaction, the complexes of NO₃⁻ anion and OAc⁻ anion are more likely to have a higher dimension. This gives us new ideas for synthetic high dimensional complexes.

Photoluminescence Studies. *Absorption properties of the ligands and the complexes in CH₃CN.* The UV–vis absorption spectra of the ligands L¹–L⁵ and the corresponding Zn(II)/Cd(II) complexes were recorded at room temperature in CH₃CN (10 μmol L⁻¹). As the ligands have similar structures, the UV–vis spectra are similar (Figure S14, Supporting Information). As shown in Figure 6, the absorption bands of the Zn(II)/Cd(II) complexes are similar to the corresponding ligands; thus, these absorption bands can be assigned to the transitions of the corresponding ligands. The UV–vis absorption spectra of these nine Zn(II)/Cd(II) complexes exhibit two distinct absorption bands in the range 250 to 500 nm ($\epsilon = 2235\text{--}42213\text{ M}^{-1}\text{ cm}^{-1}$). The numerical values of the maximum absorption wavelength and molar extinction coefficients (ϵ) are listed in Table 2. The high energy bands at *ca.* 274–289 nm are assigned to the $\pi\text{--}\pi^*$ transition of the C=N chromophore, whereas the low energy bands at *ca.* 333–359 nm are due to n- π^* transitions,^{47,48} which are in accordance with previous studies of Schiff base complexes. After complexation, these bands were shifted to a lower wavelength (hypsochromic shift) region, thus suggesting the coordination of the pyridine nitrogen and imine nitrogen with the Zn(II)/Cd(II) ions.

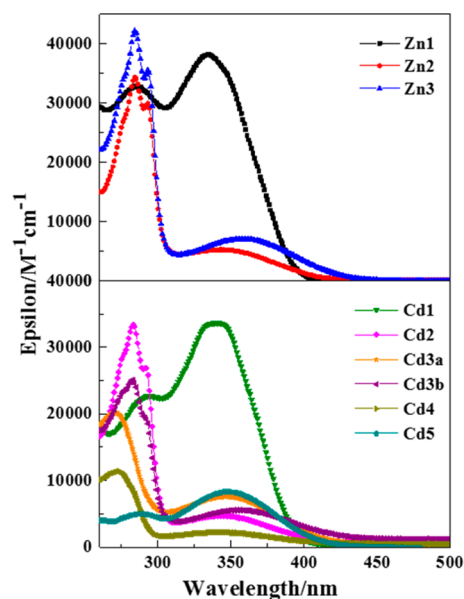


Figure 6. UV–vis absorption spectra of the complexes Zn1–Zn3, Cd1, Cd2, Cd3a, Cd3b, Cd4, and Cd5 in acetonitrile solution at room temperature.

Solid-state and solution luminescence properties of the ligands and the complexes. The d^{10} metal complexes have been reported to exhibit solid state emissions with easily modulated intensities and wavelengths.^{49–51} Hence, the luminescence properties of the ligands L¹–L⁵ and the corresponding nine Zn(II)/Cd(II) complexes were examined in the solid state at room temperature. Selected data are summarized in Table 2. The free ligands L¹–L⁵ exhibit intense emission bands centered at 474, 473, 494, 462, and 459 nm (Figure S15, Supporting Information), respectively, which may be attributed to the $\pi^*\text{--}\pi$ transitions.^{52,53} For the complexes Zn1–Zn3, Cd1, Cd2, Cd3a, Cd3b, Cd4, and Cd5, the emission bands are observed at 486, 495, 509, 489, 503, 507, 575, 483, and 485 nm (Figure 7a), respectively. These bands are red-shifted as compared to that of the corresponding ligand. Due to the similarity of the emission bands with that of the corresponding ligand, the emissions of these nine Zn(II)/Cd(II) complexes may be attributed to the intraligand transitions.^{54,55} A trend was observed in λ_{em} with Zn1 < Zn2 < Zn3 and Cd4 < Cd5 < Cd1 \approx Cd2 < Cd3a, Cd3b, which is consistent with the electron-donating ability ($-i\text{-C}_3\text{H}_7 < -\text{C}_2\text{H}_5 < -\text{CH}_3$) of substituents of these ligands L¹–L⁵. The electron-donating effect decreased the energy difference between the HOMO and LUMO, leading to a λ_{em} red-shift.⁵⁶ Although complexes Cd3a and Cd3b have the same metal ions, their emission wavelengths and intensities differ greatly, which may be ascribed to the difference in the coordinated anions, because luminescent behavior is closely related to the local environments around the metal ions.^{57,58} It is also noteworthy that the luminescence intensities for Zn1 and Cd1 are stronger than that for the others, which may be related to the better planarity and the C–H⋯O and $\pi\cdots\pi$ stacking interactions for assembled supramolecular structures in the solid state complex.⁵⁹

In acetonitrile solution, the emission bands are observed at 382–418 nm and 401–436 nm, respectively, for ligands L¹–L⁵ (Figure S16, Supporting Information) and the nine complexes (Figure 7b). These bands exhibit deep blue luminescence

Table 2. Photophysical Properties of Ligands L¹–L⁵ and Complexes Zn1–Zn3, Cd1, Cd2, Cd3a, Cd3b, Cd4, and Cd5

complex	absorption ^a		photoluminescence in acetonitrile					photoluminescence in the solid state			
	$\lambda_{\text{abs}}/\text{nm}$ ($\epsilon/\text{M}^{-1} \text{cm}^{-1}$)	$\lambda_{\text{em}}/\text{nm}$	FWHM/nm	$\tau/\mu\text{s}$	Φ_{PL}^b	CIE(x, y)	$\lambda_{\text{em}}/\text{nm}$	FWHM/nm	$\tau/\mu\text{s}$	CIE(x, y)	
L ¹	283(26774), 323(21417)	410	84.18	5.58	0.017	0.16, 0.07	474	101.71	7.71	0.18, 0.24	
Zn1	283(32794), 333(38129)	417	74.41	7.72	0.118	0.17, 0.12	486	82.53	9.92	0.20, 0.39	
Cd1	289(22247), 349(33605)	425	77.60	7.26	0.112	0.15, 0.08	489	95.05	9.12	0.21, 0.33	
L ²	274(17947), 347(4190)	412	90.58	4.25	0.027	0.21, 0.20	473	127.50	6.86	0.17, 0.23	
Zn2	283(34368), 347(5199)	434	69.79	7.99	0.254	0.17, 0.11	495	96.08	8.25	0.26, 0.37	
Cd2	283(33402), 349(4573)	433	78.75	8.17	0.210	0.18, 0.15	503	93.88	8.57	0.18, 0.40	
L ³	274(17800), 348(3725)	418	101.15	5.20	0.035	0.22, 0.21	494	159.34	6.02	0.28, 0.36	
Zn3	283(42213), 359(7023)	435	62.99	6.31	0.287	0.17, 0.11	509	108.64	7.86	0.31, 0.50	
Cd3a	274(19935), 348(7570)	430	66.48	8.05	0.190	0.18, 0.14	507	138.67	8.79	0.27, 0.41	
Cd3b	283(25086), 355(5556)	435	77.63	8.10	0.246	0.18, 0.15	575	128.31	9.52	0.47, 0.52	
L ⁴	274(16505), 342(2090)	399	64.73	4.84	0.017	0.23, 0.17	462	146.61	5.74	0.15, 0.21	
Cd4	274(11390), 346(2235)	404	60.08	5.94	0.138	0.20, 0.16	483	113.37	8.35	0.24, 0.34	
L ⁵	274(19935), 343(2590)	382	74.12	5.41	0.015	0.23, 0.22	459	147.13	5.50	0.20, 0.25	
Cd5	286(4940), 351(8235)	401	65.21	6.16	0.125	0.21, 0.18	485	116.56	7.08	0.20, 0.29	

^aMeasured in CH₃CN solutions ($\sim 1 \times 10^{-5}$ M). ^bTake quinine sulfate in 0.1 mol L⁻¹ H₂SO₄ as reference ($\Phi_{\text{PL}} = 0.546$).

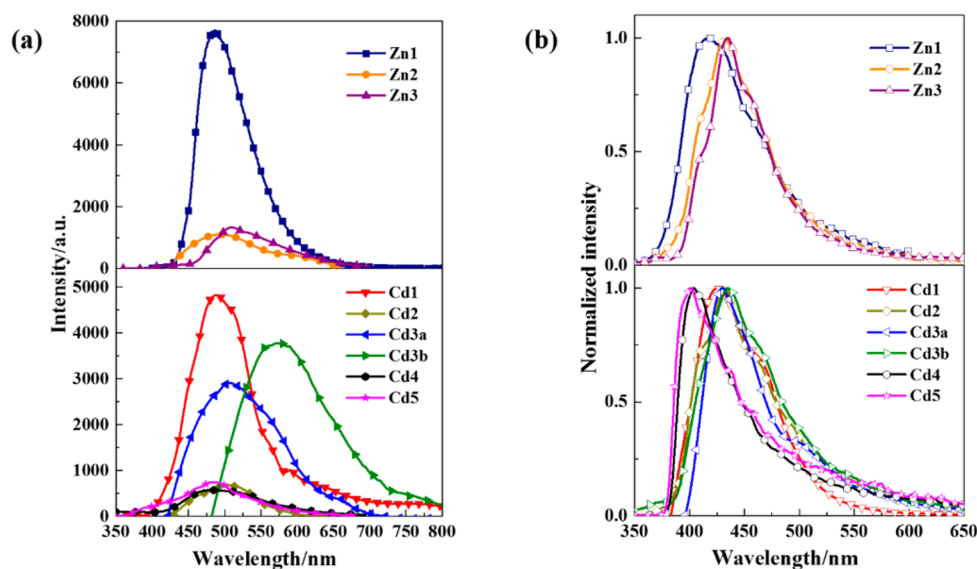


Figure 7. Emission spectra of the complexes Zn1–Zn3, Cd1, Cd2, Cd3a, Cd3b, Cd4, and Cd5 in (a) the solid state and (b) acetonitrile solution.

emission, and the Commission Internationale d'Éclairage (CIE) coordinates are summarized in Table 2. In acetonitrile solution, the maximum emission peaks are blue-shifted 61–140 nm compared with those in the solid state. These phenomena can be explained by the formation of hydrogen bonds and $\pi \cdots \pi$ stacking interactions in the solid state, which can effectively decrease the HOMO–LUMO energy gap, and influence the ligand-centered $\pi^*-\pi$ transitions.⁶⁰ Meanwhile, the full width at half-maximum (fwhm) of the emission band decreases from acetonitrile solution to the solid state (Table 2). All luminescence quantum yields of these nine Zn(II)/Cd(II) complexes in solution were measured by the optical dilute method of Demas and Crosby⁶¹ with a standard of quinine sulfate ($\Phi_{\text{r}} = 0.546$) and are listed in Table 2. The luminescence quantum yields of Zn1–Zn3, Cd1, Cd2, Cd3a, Cd3b, Cd4, and Cd5 in CH₃CN are 0.118, 0.254, 0.287, 0.112, 0.210, 0.190, 0.246, 0.138, and 0.125, respectively, which are higher than that of the corresponding ligand. Particularly, the quantum yield of Zn2 ($\Phi_{\text{r}} = 0.254$) is 9.41-fold compared to L² ($\Phi_{\text{r}} = 0.027$). This is because the coordination of the ligands to the M(II) ions increases the rigidity of the molecular edifice

and reduces the loss of energy by radiationless thermal vibrations.⁶² In addition, the quantum yields of Zn1 and Cd1 are apparently weaker than that of the other complexes in acetonitrile solution; on the contrary, they exhibit excellent luminescence emission in the solid state.

The luminescence decay profiles of ligands L¹–L⁵ and the nine Zn(II)/Cd(II) complexes were measured at their optimal excitation wavelengths in the solid state and acetonitrile solution at 298 K. The detailed data are listed in Table S6, Supporting Information. A general trend is that the luminescence lifetimes for M(II) (M = Zn and Cd) complexes either in the solid state or acetonitrile solution at 298 K are mostly longer than that of the corresponding ligands L¹–L⁵. The most obvious observation is that the lifetime of Cd2 ($\tau = 8.17 \mu\text{s}$) is 1.92-fold compared to the corresponding ligand L² ($\tau = 4.25 \mu\text{s}$) in acetonitrile solution. This is attributed to the more stable structure and interaction upon coordination.⁶³ Meanwhile, the luminescence lifetimes of the ligand and corresponding complexes in the solid state ($\tau = 5.50$ – $7.71 \mu\text{s}$ for L¹–L⁵; $\tau = 7.08$ – $9.92 \mu\text{s}$ for Zn(II)/Cd(II) complexes) are longer than those in acetonitrile solution ($\tau = 4.25$ – $5.58 \mu\text{s}$ for

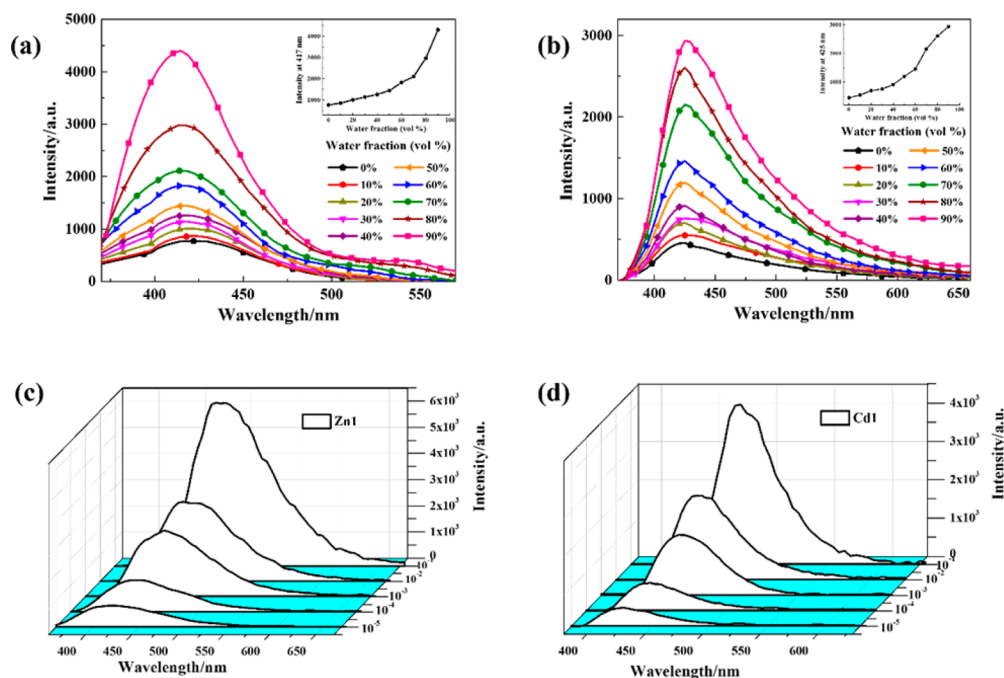


Figure 8. Emission spectra of complexes (a) **Zn1** and (b) **Cd1** ($10 \mu\text{M}$) in $\text{CH}_3\text{CN}-\text{H}_2\text{O}$ mixtures with different water fractions (0–90% v/v) at room temperature. Inset: Plot of luminescence intensity of complexes **Zn1** and **Cd1** in $\text{CH}_3\text{CN}-\text{H}_2\text{O}$ mixtures with different amounts of water. Luminescence intensities of complexes (c) **Zn1** and (d) **Cd1** in CH_3CN at different concentrations.

L^1-L^5 ; $\tau = 5.94-8.17 \mu\text{s}$ for $\text{Zn}(\text{II})/\text{Cd}(\text{II})$ complexes), which might be explained by the fact that there is a less polar nature in the solid-state environment.⁶⁴

Effect of aryl substitution and anion on luminescence properties in the solid state. In this article, we mainly talk about photoluminescence properties from two aspects: for one thing, the electron-donating ability of the alkyl substitution could regulate and control the maximum emission wavelength, and then realize the control of luminescence color. For instance, a trend was observed in λ_{em} with **Zn1** (486 nm) < **Zn2** (495 nm) < **Zn3** (509 nm) in the solid state, which is consistent with the electron-donating ability ($2,4,6-(\text{CH}_3)_3 > 2,6-(\text{CH}_3)_2 > 2-\text{CH}_3$) of substituents of ligands. As shown in Table 2, the $\text{Cd}(\text{II})$ complexes also have analogous regular pattern. For another, the anions (Cl^- , NO_3^- , OAc^-) mainly influence the intensity of emission. The emission intensities of Cl^- anion complexes are generally lower than those of NO_3^- and OAc^- anion complexes. This phenomenon indicates that the presence of chlorine on the complex skeleton induces a noticeable decrease of the intensity. Such behavior could be assigned to the heavy atom effect and suggest that they might have a higher intersystem crossing (ISC) efficiency, resulting in a decrease of the emission.

Aggregation-induced emission enhancement (AIEE) properties of complexes **Zn1 and **Cd1**.** The emission behaviors of **Zn1** and **Cd1** have been further investigated through a classical AIE experiment. We added different amounts of water, a poor solvent for the luminophors, to the pure CH_3CN solutions to obtain water fractions (f_w) of 0–90% and then monitored the photoluminescence changes. The concentration was maintained at $10 \mu\text{mol L}^{-1}$. As shown in Figures 8a and 8b, there is a clear trend that **Zn1** and **Cd1** are weakly emissive in acetonitrile solution, but the emission dramatically increased after adding a large amount of water. The emission intensity is very weak, and changes little as f_w increases from 0% to 40%.

However, a significant enhancement of luminescence is observed when the water fraction reaches 50%. The emission intensity in the $\text{CH}_3\text{CN}-\text{H}_2\text{O}$ mixture with $f_w = 90\%$ is about 5.59 and 6.45 times higher than that in pure CH_3CN solution for **Zn1** and **Cd1**, respectively, which indicates that the complexes **Zn1** and **Cd1** have AIEE activity. The inset depicts the changes of luminescence intensity with different water fractions. Compared with the emission spectrum of **Zn1** in pure CH_3CN solution, the solid emission spectrum shows a 69 nm (64 nm for **Cd1**) red-shifted emission, and the solid state emission intensity of **Zn1** becomes 10.4-fold (10.6 for **Cd1**) higher than that in pure CH_3CN solution (Figure S17, Supporting Information).

We performed another experiment: the emission spectra of **Zn1** and **Cd1** in different concentrations of CH_3CN were recorded (Figures 8c and 8d). It can be clearly seen that the CH_3CN solution with a low concentration ($c = 10^{-5} \text{ M}$) was a weak emission and the luminescence spectrum were nearly parallel to the abscissa. However, the luminescence intensities abruptly increased when the concentration was $>10^{-3} \text{ M}$. As the concentration reached 10^{-1} M , the emission intensity was approximately 7.7 and 8.7 times higher than the molecularly dispersed species in CH_3CN for **Zn1** and **Cd1**, respectively. The emission maxima were 53 nm (**Zn1**) and 50 nm (**Cd1**) red-shifted. These results indicate that these complexes are indeed a weak emitter in dilute solution, which is close to the properties described by the aggregation-induced emission concept.⁶⁵ As reported by previous literature,^{66–68} the AIEE mechanism of these complexes possibly arose from the restriction of intramolecular rotation. In the mixture of $\text{CH}_3\text{CN}/\text{H}_2\text{O}$ (10/90 v/v), most of the **Zn1** and **Cd1** molecules aggregated together rapidly by the intermolecular $\text{C}-\text{H}\cdots\text{O}$ hydrogen bonding and $\pi\cdots\pi$ stacking interactions between adjacent pyridyl rings and phenyl rings. Such free rotations are hindered and further increase the rigidity of the

molecules to generate a more extended planar skeleton; thus, this might influence the luminescence.^{69–71} Simultaneously, the complexes **Zn1** and **Cd1** have a planar conformation with minor torsion angles between the pyridyl ring and phenyl ring (6.053°/10.027° for **Zn1**; 14.226° for **Cd1**), which is beneficial for luminescence emission.⁷² Complexes with these AIEE effects can be extensively applied as solid state emission materials.

CONCLUSIONS

In summary, five Schiff base ligands (*E*)-*N*-(pyridine-2-yl)(CH=NPhR) (where R = 4-CH₃, **L**¹; 2,6-(CH₃)₂, **L**²; 2,4,6-(CH₃)₃, **L**³; 2,6-(C₂H₅)₂, **L**⁴; 2,6-(*i*-C₃H₇)₂, **L**⁵) and nine Zn(II)/Cd(II) complexes **Zn1–Zn3**, **Cd1**, **Cd2**, **Cd3a**, **Cd3b**, **Cd4**, and **Cd5** have been successfully synthesized. They are excellent models for investigating the alkyl substitution effect on the supramolecular metal–organic frameworks (SMOFs) and photoluminescence properties. The crystal structures of these complexes indicate that intermolecular interactions, such as C–H⋯O/C–H⋯Cl hydrogen bonds and π⋯π interactions, play essential roles in constructing 1D → 3D supramolecular architectures. Upon irradiation with UV light, the nine Zn(II)/Cd(II) complexes display deep blue emissions of 401–436 nm in acetonitrile solution and light blue, bluish green emissions of 485–575 nm in the solid state, respectively. The photoluminescence properties of nine Zn(II)/Cd(II) complexes can be finely and predictably tuned over a wide range of wavelengths by small and easily implemented changes to ligand structure. By modifying the phenyl moiety with electron-donating substituents, the energy difference between HOMO and LUMO decreases, and the emissions red-shift accordingly. It is worth noting that **Zn1** and **Cd1** exhibit obvious aggregation-induced emission enhancement (AIEE) properties in the CH₃CN–H₂O mixture solutions.

EXPERIMENTAL SECTION

Materials and instrumentation. All reagents and solvents were purchased from commercial sources and were used without further purification. Elemental analyses were carried out on a Perkin–Elmer 2400 automatic analyzer. FT–IR spectra data (4000–400 cm^{−1}) were collected by a Nicolet impact 410 FT–IR spectrometer. ¹H NMR spectra were obtained using a Bruker Avance–400 MHz spectrometer with Si(CH₃)₄ as internal standard. A Perkin–Elmer Lambda 35 spectrometer was used to measure the UV–vis absorption spectra of ligands and complexes. The emission luminescence and lifetime properties were recorded with Edinburgh FLS 920 fluorescence spectrometer. Lifetime studies were performed using photon-counting system with a microsecond pulse lamp as the excitation source. The emission decays were analyzed by the sum of exponential functions. The decay curve is well fitted into a double exponential function:⁷³ $I(t) = A_1 \exp(-t/\tau_1) + A_2 \exp(-t/\tau_2)$, where I is the luminescence intensity, and τ_1 and τ_2 are the lifetimes for the exponential components. The average lifetime was calculated according to the following equation:

$$\frac{\tau_1^2 A_1 \% + \tau_2^2 A_2 \%}{\tau_1 A_1 \% + \tau_2 A_2 \%} \quad (1)$$

Reference for quantum yield measurements: Lakowicz, J. R. *Principles of Fluorescence Spectroscopy*, 2nd ed.; Kluwer Academic/Plenum Publishers: New York, 1999. Quinine sulfate in 0.1 M H₂SO₄ (quantum yield 0.546 at 350 nm) was chosen as a standard.^{74,75} Absolute values are calculated using the standard reference sample that has a fixed and known fluorescence quantum yield value, according to the following equation:

$$Q = Q_R \frac{I}{I_R} \frac{OD}{OD_R} \frac{n^2}{n_R^2} \quad (2)$$

In eq 2, Q is the quantum yield, I is the measured integrated emission intensity, n is the refractive index, and OD is the optical density. The subscript R refers to the reference fluorophore of known quantum yield. In order to minimize reabsorption effects, absorbencies in the 10 mm fluorescence cuvette were kept under 0.05 at the excitation wavelength (350 nm).

X-ray crystallography. Suitable crystals of nine zinc(II)/cadmium(II) complexes **Zn1–Zn3**, **Cd1**, **Cd2**, **Cd3a**, **Cd3b**, **Cd4**, and **Cd5** were selected and mounted on a Rigaku R–AXIS RAPID IP diffractometer. Diffraction data were collected using graphite-monochromatized Mo- $K\alpha$ radiation ($\lambda = 0.71073$ Å). The structures were solved with direct methods⁷⁶ and refined with full–matrix least–squares on F^2 . All the hydrogen atoms were constrained in geometric positions to their parent atoms and non-hydrogen atoms were refined anisotropically. The detailed crystal structure refinement data are given in Table S1 (the Supporting Information), selected bond lengths and angles are listed in Tables S2–S5 (the Supporting Information). The CCDC numbers are 1449214–1449222 for **Zn1**, **Cd1**, **Zn2**, **Cd2**, **Zn3**, **Cd3a**, **Cd3b**, **Cd4**, and **Cd5**, respectively.

General synthesis of ligand. The Schiff base ligands **L**¹–**L**⁵ were synthesized by dissolving 2-pyridinecarboxaldehyde in anhydrous methanol (10 mL) and 1 molar equivalence of the respective aniline derivatives (4-methylaniline, 2,6-dimethylaniline, 2,4,6-trimethylaniline, 2,6-diethylaniline, and 2,6-diisopropylaniline) in anhydrous methanol (10 mL) and mixing the two. The resultant solutions were set at reflux for ca. 8–12 h and subsequently concentrated under reduced pressure to obtain the crude products. **L**¹ was recrystallized from the mixed solvent of *n*-hexane and dichloromethane to give yellow crystal. **L**³ and **L**⁵ were recrystallized from *n*-hexane to give yellow crystals.

(E)-4-Methyl-N-((pyridin-2-yl)methylene)aniline (L¹). 2-Pyridinecarboxaldehyde (1.52 mL, 15.98 mmol) and 4-methylaniline (1.77 mL, 15.88 mmol) were dissolved in 20 mL of anhydrous methanol and the resulting mixture was heated at reflux temperature for 3 h. The solvent was removed under reduced pressure and the residue was recrystallized from the mixed solvent of *n*-hexane and dichloromethane to give yellow crystals. Yield: 2.79 g (90%). Anal. Calcd (%) for C₁₃H₁₂N₂ ($M = 196.25$ g mol^{−1}): C, 79.56; H, 6.16; N, 14.27. Found: C, 79.55; H, 6.17; N, 14.28. FT-IR (KBr, cm^{−1}): 3429(w), 3050(w), 2917(w), 2861(w), 1628(m), 1582(m), 1566(m), 1506(s), 1463(m), 1434(m), 1347(w), 1291(w), 1256(w), 1234(w), 1213(w), 1198(w), 1140(w), 1111(w), 1085(w), 1038(w), 992(m), 969(w), 947(w), 880(m), 822(s), 774(w), 738(m), 706(w), 646(w), 617(m), 542(m), 497(w), 477(w). ¹H NMR (400 MHz, CDCl₃): δ 8.74 (d, 1H, Py-H₆), 8.65 (s, 1H, CH=N), 8.24 (d, 1H, Py-H₃), 7.84 (t, 1H, Py-H₄), 7.40 (t, 1H, Py-H₅), 6.63–7.29 (m, 4H, Ph-H_{3,4,5,6}), 2.41 (s, 3H, Ph-CH₃) ppm.

(E)-2,6-Dimethyl-N-((pyridin-2-yl)methylene)aniline (L²). 2-Pyridinecarboxaldehyde (1.50 mL, 15.77 mmol) and 2,6-dimethylaniline (1.95 mL, 15.77 mmol) gave 2.72 g of product (yield: 82%). Anal. Calcd (%) for C₁₄H₁₄N₂ ($M = 210.27$ g mol^{−1}): C, 79.97; H, 6.71; N, 13.32. Found: C, 79.90; H, 6.67; N, 13.42. FT-IR (KBr, cm^{−1}): 3434(w), 3045(w), 2916(m), 2852(w), 1652(s), 1585(m), 1568(m), 1469(s), 1436(m), 1374(w), 1348(w), 1289(w), 1252(w), 1190(s), 1146(m), 1088(m), 1041(m), 990(m), 918(w), 872(m), 829(w), 776(s), 739(w), 704(w), 630(w), 611(w), 564(w), 467(w). ¹H NMR (400 MHz, CDCl₃): δ 8.76 (d, 1H, Py-H₆), 8.38 (s, 1H, CH=N), 8.33 (d, 1H, Py-H₃), 7.88 (t, 1H, Py-H₄), 7.44 (t, 1H, Py-H₅), 7.01–7.12 (m, 3H, Ph-H_{3,4,5}), 2.20 (s, 6H, Ph-CH₃) ppm.

(E)-2,4,6-Trimethyl-N-((pyridin-2-yl)methylene)aniline (L³). 2-Pyridinecarboxaldehyde (1.50 mL, 15.75 mmol) and 2,4,6-trimethylaniline (2.22 mL, 15.81 mmol) gave 2.68 g of product (yield: 76%). Anal. Calcd (%) for C₁₅H₁₆N₂ ($M = 224.30$ g mol^{−1}): C, 80.32; H, 7.19; N, 12.49. Found: C, 80.28; H, 7.18; N, 12.45. FT-IR (KBr, cm^{−1}): 3432(w), 3050(w), 2911(m), 2854(w), 1668(vs), 1586(m), 1567(m), 1482(s), 1468(s), 1436(m), 1400(w), 1386(w), 1376(w), 1347(w), 1288(w), 1259(w), 1202(s), 1144(m), 1088(w), 1041(w), 1015(w),

993(m), 982(m), 955(w), 934(w), 897(w), 876(s), 863(s), 791(m), 770(s), 739(m), 643(w), 618(w), 577(w), 489(w). ^1H NMR (400 MHz, CDCl_3): δ 8.72 (d, 1H, Py- H_6), 8.33 (s, 1H, $\text{CH}=\text{N}$), 8.29 (d, 1H, Py- H_3), 7.84 (t, 1H, Py- H_4), 7.40 (t, 1H, Py- H_5), 6.90 (s, 2H, Ph- $H_{3,5}$), 2.14–2.29 (m, 9H, Ph- CH_2) ppm.

(E)-2,6-Diethyl-N-((pyridin-2-yl)methylene)aniline (L^4). 2-Pyridinecarboxaldehyde (1.53 mL, 16.08 mmol) and 2,6-diethylaniline (2.70 mL, 16.28 mmol) gave 3.50 g of product (yield: 91%). Anal. Calcd (%) for $\text{C}_{16}\text{H}_{18}\text{N}_2$ ($M = 238.33$ g mol $^{-1}$): C, 80.63; H, 7.61; N, 11.75. Found: C, 80.58; H, 7.63; N, 11.72. FT-IR (KBr, cm^{-1}): 3425(w), 3052(w), 2964(m), 2871(w), 1643(s), 1584(m), 1565(m), 1468(s), 1435(m), 1374(m), 1355(w), 1319(w), 1292(w), 1256(w), 1228(w), 1189(m), 1164(w), 1147(m), 1099(m), 1088(w), 1060(w), 1041(w), 1006(w), 992(m), 964(w), 875(s), 835(w), 797(w), 775(s), 753(s), 704(w), 635(w), 618(w), 593(w), 563(w), 525(w), 499(w), 471(w). ^1H NMR (400 MHz, CDCl_3): δ 8.78 (d, 1H, Py- H_6), 8.38 (s, 1H, $\text{CH}=\text{N}$), 8.32 (d, 1H, Py- H_3), 7.89 (t, 1H, Py- H_4), 7.45 (t, 1H, Py- H_5), 7.09–7.15 (m, 3H, Ph- $H_{3,4,5}$), 2.56 (q, 4H, Ph- CH_2), 1.18 (t, 6H, Ph- CH_3) ppm.

(E)-2,6-Diisopropyl-N-((pyridin-2-yl)methylene)aniline (L^5). 2-Pyridinecarboxaldehyde (1.16 mL, 12.19 mmol) was refluxed (4 h) with 2,6-diisopropylaniline (2.35 mL, 12.46 mmol) in 25 mL of anhydrous methanol. The solvent was removed under reduced pressure and the residue was purified by column chromatography using a mixture of ethyl acetate and aether petrolei (1:3, v/v) as eluent.

Recrystallization from *n*-hexane gave yellow crystals, which were filtered and washed with cold *n*-hexane. Yield: 2.28 g (70%). Anal. Calcd (%) for $\text{C}_{18}\text{H}_{22}\text{N}_2$ ($M = 266.38$ g mol $^{-1}$): C, 81.16; H, 8.32; N, 10.52. Found: C, 81.08; H, 8.36; N, 10.50. FT-IR (KBr, cm^{-1}): 3428(w), 3072(w), 2959(vs), 2867(m), 1653(s), 1587(m), 1567(m), 1471(s), 1440(m), 1385(m), 1363(m), 1347(m), 1324(m), 1308(m), 1295(m), 1254(m), 1226(w), 1179(m), 1150(m), 1107(w), 1091(w), 1054(m), 1045(m), 1011(w), 996(m), 970(w), 933(m), 879(m), 827(w), 808(w), 796(m), 779(m), 755(s), 701(w), 640(w), 620(w), 563(w), 533(w), 493(w), 459(w). ^1H NMR (400 MHz, CDCl_3): δ 8.77 (d, 1H, Py- H_6), 8.36 (s, 1H, $\text{CH}=\text{N}$), 8.32 (d, 1H, Py- H_3), 7.92 (t, 1H, Py- H_4), 7.46 (t, 1H, Py- H_5), 6.83–7.20 (m, 3H, Ph- $H_{3,4,5}$), 3.00 (q, 2H, Ph- CH), 1.21 (d, 12H, Ph- CH_3) ppm.

$[\text{Zn}_3(\text{L}^1)_2(\text{OAc})_6]$ (Zn1). A mixture of $\text{Zn}(\text{OAc})_2 \cdot 2\text{H}_2\text{O}$ (21.9 mg, 0.1 mmol) and L^1 (19.1 mg, 0.1 mmol) was dissolved in CH_3CN (8 mL) and stirred for 30 min, then heated in a sealed vial at 80 °C for 1 day. Colorless rectangular block crystals of Zn1 were obtained. Yield: 30.0 g (65%). Anal. Calcd (%) for $\text{C}_{38}\text{H}_{42}\text{O}_{12}\text{N}_4\text{Zn}_3$ ($M = 942.87$ g mol $^{-1}$): C, 48.41; H, 4.49; N, 5.94. Found: C, 48.47; H, 4.52; N, 5.92. FT-IR (KBr, cm^{-1}): 3433(w), 3029(w), 2923(w), 2870(w), 1616(m), 1509(m), 1481(m), 1424(s), 1385(m), 1322(m), 1272(w), 1243(w), 1200(w), 1178(w), 1160(w), 1104(w), 1051(m), 1019(m), 964(w), 933(w), 914(w), 838(m), 829(m), 776(m), 750(w), 681(m), 666(m), 614(m), 541(m), 426(w). ^1H NMR (400 MHz, CDCl_3): δ 8.73 (d, 1H, Py- H_6), 8.67 (s, 1H, $\text{CH}=\text{N}$), 8.16 (d, 1H, Py- H_3), 8.00 (t, 1H, Py- H_4), 7.57 (t, 1H, Py- H_5), 7.25–7.32 (m, 4H, Ph- $H_{3,4,5,6}$), 2.34 (s, 3H, Ph- CH_3), 1.82 (s, 9H, $-\text{CH}_3\text{COO}$) ppm.

$[\text{CdL}^1(\text{OAc})_2]$ (Cd1). The preparation of Cd1 was similar to that of Zn1 , except for $\text{Cd}(\text{OAc})_2 \cdot 2\text{H}_2\text{O}$ (26.7 mg, 0.1 mmol) was used instead of $\text{Zn}(\text{OAc})_2 \cdot 2\text{H}_2\text{O}$. Yield: 30.8 g (72%). Anal. Calcd (%) for $\text{C}_{17}\text{H}_{18}\text{N}_2\text{O}_4\text{Cd}$ ($M = 426.74$ g mol $^{-1}$): C, 47.85; H, 4.25; N, 6.56. Found: C, 47.78; H, 4.30; N, 6.49. FT-IR (KBr, cm^{-1}): 3403(w), 3063(w), 2981(w), 2867(w), 1626(m), 1592(s), 1563(s), 1511(m), 1481(m), 1440(m), 1414(s), 1337(m), 1312(w), 1270(w), 1239(w), 1198(w), 1158(w), 1102(w), 1051(w), 1015(m), 939(w), 910(w), 829(m), 814(m), 781(m), 747(w), 705(w), 671(s), 653(m), 635(w), 619(w), 537(m), 506(w), 485(w), 462(w), 427(w). ^1H NMR (400 MHz, CDCl_3): δ 8.98 (d, 1H, Py- H_6), 8.69 (s, 1H, $\text{CH}=\text{N}$), 8.10 (t, 1H, Py- H_3), 7.82 (d, 1H, Py- H_4), 7.72 (t, 1H, Py- H_5), 7.30–7.56 (m, 4H, Ph- $H_{3,4,5,6}$), 2.41 (s, 3H, Ph- CH_3), 2.04 (s, 6H, $-\text{CH}_3\text{COO}$) ppm.

$[\text{ZnL}^2\text{Cl}_2]$ (Zn2). L^2 (41.5 mg, 0.2 mmol) and ZnCl_2 (27.3 mg, 0.2 mmol) were refluxed in 25 mL of anhydrous methanol for 2.5 h. The mixture was then cooled to room temperature and filtered. The filtrate

was allowed to stand at room temperature in air. Yellow bulk crystals of Zn2 were obtained by slow evaporation after 1 day. Yield: 46.9 g (68%). Anal. Calcd (%) for $\text{C}_{14}\text{H}_{14}\text{Cl}_2\text{N}_2\text{Zn}$ ($M = 346.54$ g mol $^{-1}$): C, 48.52; H, 4.07; N, 8.08. Found: C, 48.55; H, 4.02; N, 8.15. FT-IR (KBr, cm^{-1}): 3434(w), 3067(w), 2955(w), 2853(w), 1631(w), 1597(s), 1569(w), 1479(m), 1444(m), 1385(w), 1359(w), 1302(m), 1275(w), 1225(w), 1184(m), 1160(w), 1106(m), 1093(w), 1071(w), 1048(w), 1024(m), 988(w), 929(w), 907(w), 788(s), 778(s), 741(w), 715(w), 648(w), 648(w), 524(w), 488(w), 435(w). ^1H NMR (400 MHz, CDCl_3): δ 8.98 (d, 1H, Py- H_6), 8.46 (s, 1H, $\text{CH}=\text{N}$), 8.32 (t, 1H, Py- H_3), 7.96 (d, 1H, Py- H_4), 7.54 (t, 1H, Py- H_5), 7.02–7.17 (m, 3H, Ph- $H_{3,4,5}$), 2.28 (s, 6H, Ph- CH_3) ppm.

$[\text{CdL}^2\text{Cl}_2]$ (Cd2). The procedure was similar to that of Zn2 , except that CdCl_2 (45.6 mg, 0.2 mmol) and CH_3CN (25 mL) were used instead of ZnCl_2 and CH_3OH , respectively. Colorless crystals of Cd2 were obtained by slow evaporation after 1 day. Yield: 43.6 g (56%). Anal. Calcd (%) for $\text{C}_{28}\text{H}_{28}\text{Cl}_4\text{N}_4\text{Cd}_2$ ($M = 787.16$ g mol $^{-1}$): C, 42.72; H, 3.59; N, 7.12. Found: C, 42.68; H, 3.63; N, 7.15. FT-IR (KBr, cm^{-1}): 3432(w), 3061(w), 2940(w), 2855(w), 1642(s), 1593(s), 1573(w), 1473(m), 1445(m), 1381(w), 1361(w), 1304(m), 1275(w), 1258(w), 1224(w), 1186(s), 1164(w), 1105(w), 1090(w), 1051(w), 1034(w), 1016(m), 984(w), 908(m), 796(s), 771(s), 741(w), 715(w), 640(w), 628(w), 520(w), 476(w), 432(w). ^1H NMR (400 MHz, CDCl_3): δ 8.83 (d, 1H, Py- H_6), 8.41 (s, 1H, $\text{CH}=\text{N}$), 8.00 (d, 1H, Py- H_3), 7.91 (t, 1H, Py- H_4), 7.54 (t, 1H, Py- H_5), 6.75–7.00 (m, 3H, Ph- $H_{3,4,5}$), 2.26 (s, 6H, Ph- CH_3) ppm.

$[\text{ZnL}^3\text{Cl}_2]$ (Zn3). The procedure was similar to that of Zn2 , except that L^3 (44.5 mg, 0.2 mmol) was used instead of L^2 . Pale yellow bulk crystals of Zn3 were obtained by slow evaporation after 3 days. Yield: 44.2 g (62%). Anal. Calcd (%) for $\text{C}_{15}\text{H}_{16}\text{Cl}_2\text{N}_2\text{Zn}$ ($M = 360.57$ g mol $^{-1}$): C, 49.96; H, 4.47; N, 7.77. Found: C, 49.88; H, 4.45; N, 7.76. FT-IR (KBr, cm^{-1}): 3438(w), 3064(w), 2920(w), 2858(w), 1629(m), 1595(s), 1568(w), 1481(s), 1444(m), 1424(w), 1383(w), 1360(m), 1301(m), 1274(w), 1227(w), 1199(m), 1161(w), 1142(w), 1106(w), 1052(w), 1025(m), 987(w), 959(w), 936(w), 908(w), 848(m), 778(s), 747(w), 731(w), 643(m), 581(w), 507(w), 497(w), 475(w), 454(w). ^1H NMR (400 MHz, CDCl_3): δ 8.97 (d, 1H, Py- H_6), 8.43 (s, 1H, $\text{CH}=\text{N}$), 8.30 (t, 1H, Py- H_3), 7.93–7.96 (m, 2H, Py- $H_{4,5}$), 6.97 (s, 2H, Ph- $H_{3,5}$), 2.26–2.33 (m, 9H, Ph- CH_3) ppm.

$[\text{CdL}^3\text{Cl}_2]$ (Cd3a). The procedure was similar to that of Zn3 , except that CdCl_2 (45.6 mg, 0.2 mmol) and CH_3OH (5 mL)/ CH_2Cl_2 (25 mL) were used instead of ZnCl_2 and CH_3OH , respectively. Yellow bulk crystals of Cd3 were obtained by slow evaporation after 2 days. Yield: 52.1 g (64%). Anal. Calcd (%) for $\text{C}_{30}\text{H}_{32}\text{Cl}_4\text{N}_4\text{Cd}_2$ ($M = 815.20$ g mol $^{-1}$): C, 44.20; H, 3.96; N, 6.87. Found: C, 44.25; H, 4.03; N, 6.85. FT-IR (KBr, cm^{-1}): 3443(m), 3066(w), 2916(w), 2860(w), 1645(s), 1594(s), 1572(w), 1484(m), 1445(m), 1383(w), 1367(w), 1311(m), 1269(w), 1229(w), 1201(w), 1162(w), 1143(m), 1104(w), 1054(w), 1040(w), 1018(m), 982(w), 969(w), 935(w), 902(m), 869(w), 853(w), 780(s), 742(w), 639(m), 584(w), 495(w), 422(w). ^1H NMR (400 MHz, CDCl_3): δ 8.84 (d, 1H, Py- H_6), 8.39 (s, 1H, $\text{CH}=\text{N}$), 8.12 (t, 1H, Py- H_3), 7.92 (t, 1H, Py- H_4), 7.56 (t, 1H, Py- H_5), 6.91 (s, 2H, Ph- $H_{3,5}$), 2.23–2.27 (m, 9H, Ph- CH_3) ppm.

$[\text{Cd}(\text{L}^3)_2(\text{NO}_3)_2]$ (Cd3b). A mixture of $\text{Cd}(\text{NO}_3)_2 \cdot 4\text{H}_2\text{O}$ (32.0 mg, 0.1 mmol) and L^3 (65.0 mg, 0.3 mmol) with a molar ratio of 1:3 was dissolved in CH_3CN (8.0 mL). After stirring for 30 min in air, it was transferred into a 15 mL Teflon-lined stainless steel autoclave and heated at 120 °C for 4.5 days. Colorless crystals of Cd3b were obtained by slow evaporation after 6 days. Yield: 46.4 g (65%). Anal. Calcd (%) for $\text{C}_{30}\text{H}_{32}\text{N}_6\text{O}_6\text{Cd}$ ($M = 685.02$ g mol $^{-1}$): C, 52.60; H, 4.71; N, 12.27. Found: C, 52.59; H, 4.75; N, 12.30. FT-IR (KBr, cm^{-1}): 3473(w), 3079(w), 2937(w), 2848(w), 2395(m), 2291(w), 1633(m), 1589(m), 1467(m), 1419(m), 1307(s), 1197(w), 1139(w), 1022(w), 904(w), 860(w), 777(w), 628(w), 590(w), 493(w), 460(w). ^1H NMR (400 MHz, CDCl_3): δ 8.85 (d, 1H, Py- H_6), 8.40 (s, 1H, $\text{CH}=\text{N}$), 8.01 (d, 1H, Py- H_3), 7.93 (t, 1H, Py- H_4), 7.57 (t, 1H, Py- H_5), 7.12 (s, 2H, Ph- $H_{3,5}$), 2.48–2.72 (m, 9H, Ph- CH_3) ppm.

$[\text{CdL}^4\text{Cl}_2]$ (Cd4). The procedure was similar to that of Cd3 , except that L^4 (23.5 mg, 0.1 mmol) was used instead of L^3 . Yellow bulk crystals of Cd3 were obtained by slow evaporation after 8 days. Yield:

29.2 g (70%). Anal. Calcd (%) for $C_{16}H_{18}Cl_2N_2Cd$ ($M = 421.62$ g mol $^{-1}$): C, 45.58; H, 4.30; N, 6.64. Found: C, 45.61; H, 4.25; N, 6.63. FT-IR (KBr, cm $^{-1}$): 3432(w), 3061(w), 2971(m), 2869(w), 1639(m), 1593(s), 1571(w), 1481(w), 1457(m), 1441(w), 1369(w), 1307(m), 1270(w), 1224(w), 1176(m), 1158(w), 1103(m), 1056(w), 1034(w), 1017(m), 987(w), 910(m), 869(w), 835(w), 808(m), 779(s), 761(w), 712(w), 640(w), 589(w), 573(w), 503(w), 439(w). 1H NMR (400 MHz, $CDCl_3$): δ 8.76 (d, 1H, Py- H_6), 8.40 (s, 1H, CH=N), 8.21 (d, 1H, Py- H_3), 8.06 (t, 1H, Py- H_4), 7.64 (t, 1H, Py- H_5), 7.03–7.12 (m, 3H, Ph- $H_{3,4,5}$), 2.46 (q, 4H, Ph- CH_2 -), 1.14 (t, 6H, Ph- CH_3) ppm.

[CdL^5Cl_2] (**Cd5**). The procedure was similar to that of **Cd4**, except that L^5 (26.6 mg, 0.1 mmol) was used instead of L^4 . Yellow bulk crystals of **Cd5** were obtained by slow evaporation after 6 days. Yield: 32.5 g (72%). Anal. Calcd (%) for $C_{18}H_{22}Cl_2N_2Cd$ ($M = 449.68$ g mol $^{-1}$): C, 48.08; H, 4.93; N, 6.23. Found: C, 48.13; H, 4.90; N, 6.25. FT-IR (KBr, cm $^{-1}$): 3448(w), 3070(w), 2965(m), 2868(w), 1640(m), 1595(s), 1572(w), 1482(m), 1458(m), 1444(m), 1384(w), 1371(w), 1330(w), 1308(w), 1270(w), 1257(w), 1223(w), 1176(m), 1158(w), 1103(m), 1058(w), 1018(m), 961(w), 933(w), 906(w), 806(s), 776(s), 761(s), 706(w), 638(w), 568(w), 539(w), 500(w), 471(w), 431(w). 1H NMR (400 MHz, $CDCl_3$): δ 8.77 (d, 1H, Py- H_6), 8.39 (s, 1H, CH=N), 8.23 (d, 1H, Py- H_3), 8.04 (t, 1H, Py- H_4), 7.63 (t, 1H, Py- H_5), 7.11–7.20 (m, 3H, Ph- $H_{3,4,5}$), 2.89 (q, 2H, Ph- CH_2 -), 1.14 (d, 12H, Ph- CH_3) ppm.

■ ASSOCIATED CONTENT

Supporting Information

The Supporting Information is available free of charge on the ACS Publications website at DOI: 10.1021/acs.cgd.6b00347.

Structural information for **Zn1–Zn3**, **Cd1**, **Cd2**, **Cd3a**, **Cd3b**, **Cd4**, and **Cd5**, FT-IR spectra, 1H NMR spectra, luminescent data, and selected bond lengths and angles for **Zn1–Zn3**, **Cd1**, **Cd2**, **Cd3a**, **Cd3b**, **Cd4**, and **Cd5** (PDF)

Accession Codes

CCDC 1449214–1449222 contain the supplementary crystallographic data for this paper. These data can be obtained free of charge via www.ccdc.cam.ac.uk/data_request/cif, or by emailing data_request@ccdc.cam.ac.uk, or by contacting The Cambridge Crystallographic Data Centre, 12 Union Road, Cambridge CB2 1EZ, UK; fax: +44 1223 336033.

■ AUTHOR INFORMATION

Corresponding Authors

*(Rui-Qing Fan) Fax: +86-451-86413710. E-mail: fanruiqing@hit.edu.cn.

*(Yu-Lin Yang) Fax: +86-451-86413710. E-mail: ylyang@hit.edu.cn.

Notes

The authors declare no competing financial interest.

■ ACKNOWLEDGMENTS

This work was supported by National Natural Science Foundation of China (Grant 21371040, 21571042, and 21171044) and the National Key Basic Research Program of China (973 Program, No. 2013CB632900).

■ REFERENCES

- Hiratani, K.; Albrecht, M. *Chem. Soc. Rev.* **2008**, *37*, 2413–2421.
- Pluth, M. D.; Bergman, R. G.; Raymond, K. N. *Acc. Chem. Res.* **2009**, *42*, 1650–1659.
- Barnett, S. A.; Champness, N. R. *Coord. Chem. Rev.* **2003**, *246*, 145–168.

(4) Han, L. L.; Hu, T. P.; Mei, K.; Guo, Z. M.; Yin, C.; Wang, Y. X.; Zheng, J.; Wang, X. P.; Sun, D. *Dalton Trans.* **2015**, *44*, 6052–6061.

(5) Banerjee, R.; Phan, A.; Wang, B.; Knobler, C.; Furukawa, H.; O’Keeffe, M.; Yaghi, O. M. *Science* **2008**, *319*, 939–943.

(6) Lin, J. B.; Zhang, J. P.; Chen, X. M. *J. Am. Chem. Soc.* **2010**, *132*, 6654–6656.

(7) Yuan, S.; Deng, Y. K.; Sun, D. *Chem. - Eur. J.* **2014**, *20*, 10093–10098.

(8) Guo, Z. Q.; Yiu, S. M.; Chan, M. C. W. *Chem. - Eur. J.* **2013**, *19*, 8937–8947.

(9) Zhou, H. C.; Long, J. R.; Yaghi, O. M. *Chem. Rev.* **2012**, *112*, 673–674.

(10) Lu, W. G.; Wei, Z. W.; Gu, Z. Y.; Liu, T. F.; Park, J.; Park, J.; Tian, J.; Zhang, M. W.; Zhang, Q.; Gentle, T., III; Bosch, M.; Zhou, H. C. *Chem. Soc. Rev.* **2014**, *43*, 5561–5593.

(11) Ali, A.; Hundal, G.; Gupta, R. *Cryst. Growth Des.* **2012**, *12*, 1308–1319.

(12) Duong, A.; Maris, T.; Wuest, J. D. *Inorg. Chem.* **2011**, *50*, 5605–5618.

(13) Natale, D.; Mareque-Rivas, J. C. *Chem. Commun.* **2008**, 425–437.

(14) Nishio, M. *CrystEngComm* **2004**, *6*, 130–158.

(15) Janssen, F. F. B. J.; Gelder, R.; Rowan, A. E. *Cryst. Growth Des.* **2011**, *11*, 4326–4333.

(16) Field, J. S.; Munro, O. Q.; Waldron, B. P. *Dalton Trans.* **2012**, *41*, 5486–5496.

(17) Lin, J. M.; Qiu, Y. X.; Chen, W. B.; Yang, M.; Zhou, A. J.; Dong, W.; Tian, C. E. *CrystEngComm* **2012**, *14*, 2779–2786.

(18) He, L.; Ma, D.; Duan, L.; Wei, Y.; Qiao, J.; Zhang, D.; Dong, G.; Wang, L.; Qiu, Y. *Inorg. Chem.* **2012**, *51*, 4502–4510.

(19) Semeniuc, R. F.; Reamer, T. J.; Smith, M. D. *New J. Chem.* **2010**, *34*, 439–452.

(20) Luo, J.; Xie, Z.; Lam, J. W.; Cheng, L.; Chen, H.; Qiu, C.; Kwok, H. S.; Zhan, X.; Liu, Y.; Zhu, D.; Tang, B. Z. *Chem. Commun.* **2001**, 1740–1741.

(21) Bhattacharya, B.; Haldar, R.; Maity, D. K.; Maji, T. K.; Ghoshal, D. *CrystEngComm* **2015**, *17*, 3478–3486.

(22) Papaefstathiou, G. S.; MacGillivray, L. R. *Coord. Chem. Rev.* **2003**, *246*, 169–184.

(23) Kuzu, I.; Krummenacher, I.; Meyer, J.; Armbruster, F.; Breher, F. *Dalton Trans.* **2008**, 5836–5865.

(24) Khavasi, H. R.; Salimi, A. R.; Eshtiagh-Hosseini, H.; Amini, M. M. *CrystEngComm* **2011**, *13*, 3710–3717.

(25) Li, G. F.; Ren, X. Y.; Shan, G. G.; Che, W. L.; Zhu, D. X.; Yan, L. K.; Su, Z. M.; Bryce, M. R. *Chem. Commun.* **2015**, *51*, 13036–13039.

(26) Nath, M.; Saini, P. K. *Dalton Trans.* **2011**, *40*, 7077–7121.

(27) Lo, W. K.; Wong, W. K.; Wong, W. Y.; Guo, J. P. *Eur. J. Inorg. Chem.* **2005**, *2005*, 3950–3954.

(28) Bassanetti, I.; Mezzadri, F.; Comotti, A.; Sozzani, P.; Gennari, M.; Calestani, G.; Marchiò, L. *J. Am. Chem. Soc.* **2012**, *134*, 9142–9145.

(29) Song, L. S.; Wang, H. M.; Niu, Y. Y.; Hou, H. W.; Zhu, Y. *CrystEngComm* **2012**, *14*, 4927–4938.

(30) Li, S. M.; Zheng, X. J.; Yuan, D. Q.; Ablet, A.; Jin, L. P. *Inorg. Chem.* **2012**, *51*, 1201–1203.

(31) Tanabe, K. K.; Allen, C. A.; Cohen, S. M. *Angew. Chem., Int. Ed.* **2010**, *49*, 9730–9733.

(32) Feng, R.; Jiang, F. L.; Chen, L.; Yan, C. F.; Wu, M. Y.; Hong, M. C. *Chem. Commun.* **2009**, 5296–5298.

(33) Wang, H. L.; Qi, D. D.; Xie, Z.; Cao, W.; Wang, K.; Shang, H.; Jiang, J. Z. *Chem. Commun.* **2013**, *49*, 889–891.

(34) Machura, B.; Nawrot, I.; Michalik, K. *Polyhedron* **2011**, *30*, 2619–2626.

(35) Ma, Q.; Zhu, M. L.; Yuan, C. X.; Feng, S. S.; Lu, L. P.; Wang, Q. M. *Cryst. Growth Des.* **2010**, *10*, 1706–1714.

(36) Liu, X. H.; Zhao, L. M.; Liu, F. S. *Acta Crystallogr., Sect. E: Struct. Rep. Online* **2012**, *E68*, m311.

- (37) Basu Baul, T. S.; Kundu, S.; Linden, A.; Raviprakash, N.; Mannac, S. K.; da Silva, M. F. C. G. *Dalton Trans.* **2014**, *43*, 1191–1202.
- (38) Roy, A. S.; Saha, P.; Mitra, P.; Maity, S. S.; Ghoshc, S.; Ghosh, P. *Dalton Trans.* **2011**, *40*, 7375–7384.
- (39) Baran, P.; Boca, R.; Breza, M.; Elias, H.; Fuess, H.; Jorik, V.; Klement, R.; Svoboda, I. *Polyhedron* **2002**, *21*, 1561–1571.
- (40) Gong, X.; Ge, Y. Y.; Fang, M.; Gu, Z. G.; Zheng, S. R.; Li, W. S.; Hu, S. J.; Li, S. B.; Cai, Y. P. *CrystEngComm* **2011**, *13*, 6911–6915.
- (41) Shakir, M.; Azam, M.; Azim, Y.; Parveen, S.; Khan, A. U. *Polyhedron* **2007**, *26*, 5513–5518.
- (42) Kumar, J.; Sarma, M. J.; Phukan, P.; Das, D. K. *Dalton Trans.* **2015**, *44*, 4576–4581.
- (43) Dong, Y. W.; Fan, R. Q.; Wang, P.; Wei, L. G.; Wang, X. M.; Zhang, H. J.; Gao, S.; Yang, Y. L.; Wang, Y. L. *Dalton Trans.* **2015**, *44*, 5306–5322.
- (44) Addison, A. W.; Rao, T. N.; Reedijk, J.; van Rijn, J.; Verschoor, G. C. *J. Chem. Soc., Dalton Trans.* **1984**, 1349–1356.
- (45) Yang, L.; Powell, D. R.; Houser, R. P. *Dalton Trans.* **2007**, 955–964.
- (46) Dong, Y. W.; Fan, R. Q.; Wang, P.; Wei, L. G.; Wang, X. M.; Gao, S.; Zhang, H. J.; Yang, Y. L.; Wang, Y. L. *Inorg. Chem.* **2015**, *54*, 7742–7752.
- (47) Dey, D.; Kaur, G.; Ranjani, A.; Gayathri, L.; Chakraborty, P.; Adhikary, J.; Pasan, J.; Dhanasekaran, D.; Choudhury, A. R.; Akbarsha, M. A.; Kole, N.; Biswas, B. *Eur. J. Inorg. Chem.* **2014**, *2014*, 3350–3358.
- (48) Maiti, M.; Sadhukhan, D.; Thakurta, S.; Roy, S.; Pilet, G.; Butcher, R. J.; Nonat, A.; Charbonnière, L. J.; Mitra, S. *Inorg. Chem.* **2012**, *51*, 12176–12187.
- (49) Wu, G.; Wang, X. F.; Okamura, T.; Sun, W. Y.; Ueyama, N. *Inorg. Chem.* **2006**, *45*, 8523–8532.
- (50) Ciurtin, D. M.; Pschirer, N. G.; Smith, M. D.; Bunz, U. H. F.; zur Loye, H. C. *Chem. Mater.* **2001**, *13*, 2743–2745.
- (51) Dong, Y. B.; Wang, P.; Huang, R. Q.; Smith, M. D. *Inorg. Chem.* **2004**, *43*, 4727–4739.
- (52) Ding, C. X.; Rui, X.; Wang, C.; Xie, Y. S. *CrystEngComm* **2014**, *16*, 1010–1019.
- (53) Shi, X.; Zhu, G. S.; Fang, Q. R.; Wu, G.; Tian, G.; Wang, R. W.; Zhang, D. L.; Xue, M.; S. Qiu, L. *Eur. J. Inorg. Chem.* **2004**, *2004*, 185–191.
- (54) Xu, C. Y.; Guo, Q. Q.; Wang, X. J.; Hou, H. W.; Fan, Y. T. *Cryst. Growth Des.* **2011**, *11*, 1869–1879.
- (55) Dong, B. X.; Xu, Q. *Cryst. Growth Des.* **2009**, *9*, 2776–2782.
- (56) Wu, Y. H.; Chen, L.; Yu, J.; Tong, S. L.; Yan, Y. *Dyes Pigm.* **2013**, *97*, 423–428.
- (57) Wen, L. L.; Dang, D. B.; Duan, C. Y.; Li, Y. Z.; Tian, Z. F.; Meng, Q. J. *Inorg. Chem.* **2005**, *44*, 7161–7170.
- (58) Zhang, Y. N.; Liu, P.; Wang, Y. Y.; Wu, L. Y.; Pang, L. Y.; Shi, Q. Z. *Cryst. Growth Des.* **2011**, *11*, 1531–1541.
- (59) Jin, F.; Wang, H. Z.; Zhang, Y.; Wang, Y.; Zhang, J.; Kong, L.; Hao, F. Y.; Yang, J. X.; Wu, J. Y.; Tian, Y. P.; Zhou, H. P. *CrystEngComm* **2013**, *15*, 3687–3695.
- (60) Stylianou, K. C.; Heck, R.; Chong, S. Y.; Bacsa, J.; Jones, J. T. A.; Khimyak, Y. Z.; Bradshaw, D.; Rosseinsky, M. J. *J. Am. Chem. Soc.* **2010**, *132*, 4119–4130.
- (61) Crosby, G. A.; Demas, J. N. *J. Phys. Chem.* **1971**, *75*, 991–1024.
- (62) Maxim, C.; Tuna, F.; Madalan, A. M.; Avarvari, N.; Andruh, M. *Cryst. Growth Des.* **2012**, *12*, 1654–1665.
- (63) Mandal, H.; Chakraborty, S.; Ray, D. *RSC Adv.* **2014**, *4*, 65044–65055.
- (64) Durai Murugan, K.; Natarajan, P. *Eur. Polym. J.* **2011**, *47*, 1664–1675.
- (65) Wang, X. M.; Wang, P.; Fan, R. Q.; Xu, M. Y.; Qiang, L. S.; Wei, L. G.; Yang, Y. L.; Wang, Y. L. *Dalton Trans.* **2015**, *44*, 5179–5190.
- (66) Hong, Y. N.; Lam, J. W. Y.; Tang, B. Z. *Chem. Commun.* **2009**, 4332–4353.
- (67) Shellaiah, M.; Wu, Y. H.; Singh, A.; Raju, M. V. R.; Lin, H. C. *J. Mater. Chem. A* **2013**, *1*, 1310–1318.
- (68) Yang, X. D.; Chen, X. L.; Lu, X. D.; Yan, C. G.; Xu, Y. K.; Hang, X. D.; Qu, J. Q.; Liu, R. Y. *J. Mater. Chem. C* **2016**, *4*, 383–390.
- (69) Zhou, T. L.; Li, F.; Fan, Y.; Song, W. F.; Mu, X. Y.; Zhang, H. Y.; Wang, Y. *Chem. Commun.* **2009**, 3199–3201.
- (70) Würthner, F.; Kaiser, T. E.; Saha-Möller, C. R. *Angew. Chem., Int. Ed.* **2011**, *50*, 3376–3410.
- (71) Wong, W. Y.; Liu, L.; Shi, J. X. *Angew. Chem., Int. Ed.* **2003**, *42*, 4064–4068.
- (72) Yang, M. D.; Xu, D. L.; Xi, W. G.; Wang, L. K.; Zheng, J.; Huang, J.; Zhang, J. Y.; Zhou, H. P.; Wu, J. Y.; Tian, Y. P. *J. Org. Chem.* **2013**, *78*, 10344–10359.
- (73) Chen, S.; Wu, Y. K.; Zhao, Y.; Fang, D. N. *RSC Adv.* **2015**, *5*, 72009–72018.
- (74) Lakowicz, R. Z. *Principles of fluorescence spectroscopy*, 2nd ed.; Klumer Academic/Plenum Publisher: New York, 1999.
- (75) Liu, H.; Ye, T.; Mao, C. *Angew. Chem., Int. Ed.* **2007**, *46*, 6473–6475.
- (76) Sheldrick, G. M. *SHELXTL NT Crystal Structure Analysis Package*, Version 5.10; Bruker AXS: Analytical X-ray System, Madison, WI, 1999.